INTERNATIONAL GEOLOGY REVIEW, 2016
VOL. 58, NO. 8, 1020–1040
http://dx.doi.org/10.1080/00206814.2015.1118647

Taylor & Francis
Taylor & Francis Group

Petrogenesis and $^{40}Ar/^{39}Ar$ dating of proto-forearc crust in the Early Cretaceous Caribbean arc: The La Tinta mélange (eastern Cuba) and its easterly correlation in Hispaniola

Concepción Lázaro[a], Idael F. Blanco-Quintero[b], Joaquin A. Proenza[c], Yamirka Rojas-Agramonte[d,e], Franz Neubauer[f], Kenya Núñez-Cambra[g] and Antonio Garcia-Casco[a,h]

[a]Departamento de Mineralogía y Petrología, Universidad de Granada, Granada, Spain; [b]Departamento de Geociencias, Universidad de los Andes, Bogotá, Colombia; [c]Departament Cristal•lografia, Mineralogia i Dipòsits Minerals, Universitat de Barcelona, Barcelona, Spain; [d]Institut für Geowissenschaften, Universität Mainz, Mainz, Germany; [e]Departamento de Ciencias de la Tierra y de la Construcción, Universidad de las Fuerzas Armadas ESPE, Sangolquì, Ecuador; [f]Fachbereich Geographie und Geologie, Universität Salzburg, Salzburg, Austria; [g]Instituto de Geología y Paleontología, Ciudad Habana, Cuba; [h]Instituto Andaluz de Ciencias de la Tierra, CSIC-Universidad de Granada, Granada, Spain

ABSTRACT

The La Tinta mélange is a small but singular ultramafic mélange sheet that crops out in eastern Cuba. It is composed of dolerite-derived amphibolite blocks embedded in a serpentinite matrix. The amphibolite blocks have mid-ocean ridge basalt (MORB)-like composition showing little if any imprint of subduction zone component, similar to most forearc and MOR basalts worldwide. Relict Cr-spinel and olivine mineral chemistry of the serpentinized ultramafic matrix suggest a forearc position for these rocks. These characteristics, together with a hornblende $^{40}Ar/^{39}Ar$ age of 123.2 ± 2.2 Ma from one of the amphibolite blocks, suggest that the protoliths of the amphibolite blocks correspond to forearc basalt (FAB)-related rocks that formed during the earlier stage of subduction initiation of the Early Cretaceous Caribbean arc. We propose that the La Tinta amphibolites correspond to fragments of sills and dikes of hypoabyssal rocks formed in the earlier stages of a subduction initiation scenario in the Pacific realm (ca. 136 Ma). The forearc dolerite-derived amphibolites formed by partial melting of upwelling fertile asthenosphere at the beginning of subduction of the Proto-Caribbean (Atlantic) slab, with no interaction with slab-derived fluids/melts. This magmatic episode probably correlates with Early Cretaceous basic rocks described in Hispaniola (Gaspar Hernandez serpentinized peridotite-tectonite). The dikes and sills cooled and metamorphosed due to hydration at low pressure (ca. 3.8 kbar) and medium to high temperature (up to 720ºC) and reached ca. 500ºC at ca. 123 Ma. At this cooling stage, serpentinite formed after hydration of the ultramafic upper mantle. This process might have been favoured by faulting during extension of the forearc, indicating an early stage of dike and sill fragmentation and serpentinite mélanges formation; however, full development of the mélange likely took place during tectonic emplacement (obduction) onto the thrust belt of eastern Cuba during the latest Cretaceous.

ARTICLE HISTORY
Received 30 July 2015
Accepted 20 October 2015

KEYWORDS
Serpentinite mélange; amphibolite; $^{40}Ar/^{39}Ar$ dating; Caribbean arc; eastern Cuba; forearc basalts

1. Introduction

'Forearc basalts' (FABs) were first defined as tholeiitic basic magmas slightly older than the thin overlying boninites that occur in the Izu–Bonin–Marianas forearc (Reagan *et al*. 2010). In an undeformed forearc sequence, gabbroic rocks occur below the FAB and above the mantle peridotites (Ishizuka *et al*. 2011). FAB lavas and related dikes have chemical composition similar to mid-ocean ridge basalt (MORB) (Reagan *et al*. 2010; Ishizuka *et al*. 2014; Pearce 2014), although the former usually present lower TiO_2 (<1–1.5 wt.%) and slight depletion in high field strength elements (HFSEs, e.g. Nb, Ta), indicating a light subduction component. Light rare earth elements (LREEs) depletion is also significant both in FAB and in MORB. Otherwise, normal island arc tholeiitic (IAT) basalts do not exhibit such characteristics. The typical island arc basalts display low TiO_2 contents and significant depletions in HFSEs relative to LREEs. Enrichment in mobile elements, such as large ion lithophile elements (LILEs, including LREEs), is also one characteristic (Pearce 2003).

In ophiolitic complexes, MORB-type basic rocks are commonly characterized as FABs that erupted during the early stages of the subduction initiation processes (Stern *et al*. 2012) or as backarc basin basalts (BABBs) that erupt much farther away from the trench (Pearce and Stern 2006). The geochemical differences between BABB and FAB are subtle. Basically, the location of BABB, further away from the trench, typically makes them carry a deep

CONTACT Concepción Lázaro clazaro@ugr.es
Supplemental data for this article can be accessed here.

subduction signal, rather than a shallow one (e.g. low H/Th, Pearce 2014). Moreover, BABBs also lack the up-sequence transition into boninites that is representative of forearc settings.

In the Caribbean realm (Figure 1(a)), Early Cretaceous boninites and boninitic gabbros and low-Ti IAT have been described in central Cuba (Fonseca *et al*. 1989; Kerr *et al*. 1999); in the Puerto Plata, Maimón, Amina, and Los Ranchos complexes, in Hispaniola (Horan 1995; Kerr *et al*. 1999; Lewis *et al*. 2000, 2002; Escuder-Viruete *et al*. 2006, 2007, 2014; Jolly and Lidiak 2006; Torró et al. 2015a, 2015b) and the Water Island Formation that crops out in the Virgin Islands (Jolly and Lidiak 2006). FABs have been recently described in basaltic rocks of the Maimón Formation (Central Cordillera, Hispaniola; Torró et al. 2015a, 2015b). These rocks represent the earliest products of the volcanic arc of the Caribbean, which formed during subduction initiation along a collapsed transform of the Proto-Caribbean oceanic basin under the Caribbean plate at 135–130 Ma (Rojas-Agramonte *et al*. 2011; Pindell *et al*. 2012; Whattam and Stern 2015). In eastern Cuba, the Mayarí-Cristal Ophiolite Massif has been interpreted as formed in a forearc (Gervilla *et al*. 2005; Proenza *et al*. 2006; Blanco-Quintero *et al*. 2011a), and also in an axial arc environment (Marchesi *et al*. 2006). On the other hand, the Moa-Baracoa Ophiolite Massif is interpreted as formed in a backarc to intra-arc environment (Proenza *et al*. 1999, 2006; Gervilla *et al*. 2005; Marchesi *et al*. 2006, 2007; Blanco-Quintero *et al*.

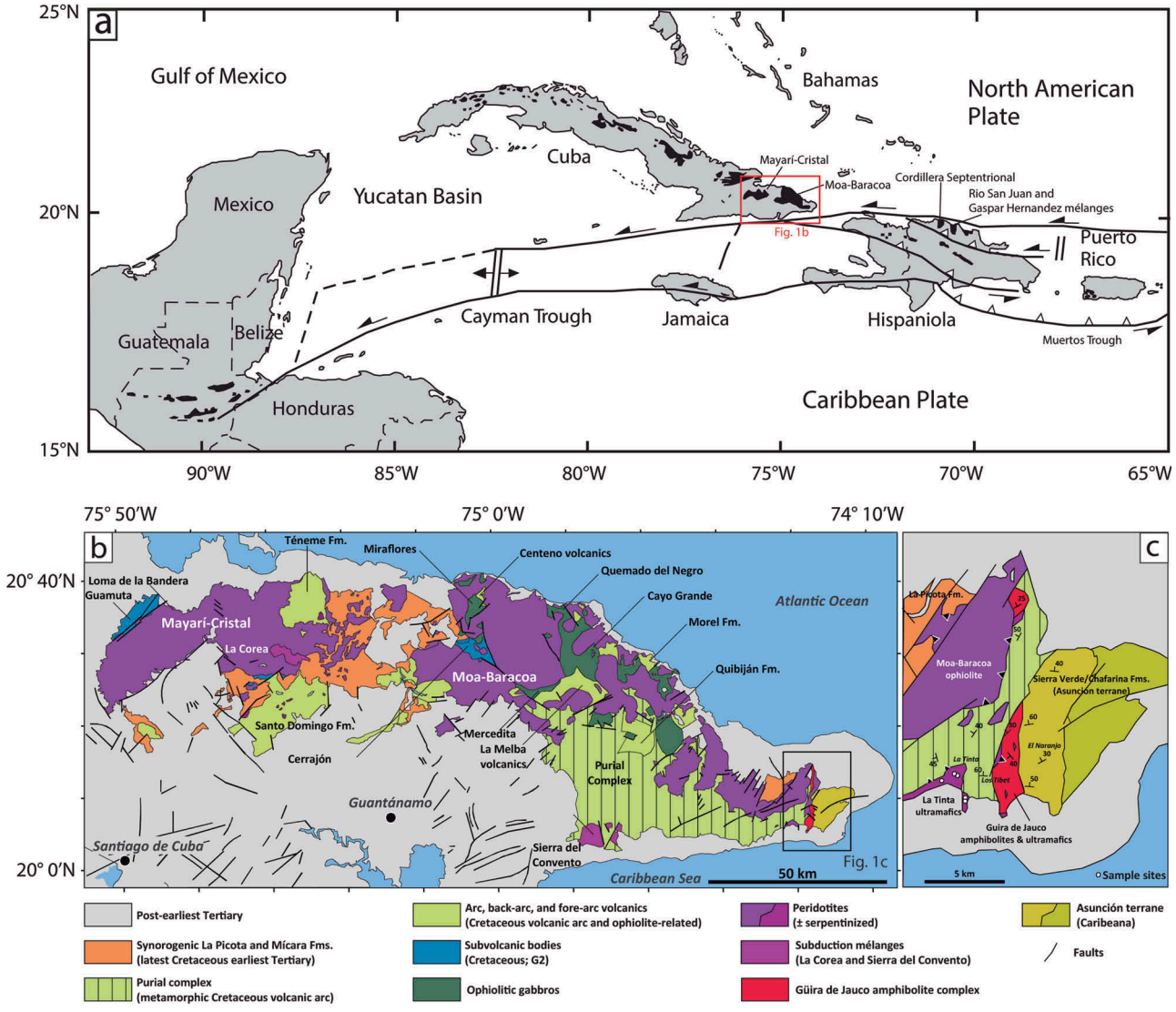

Figure 1. (a) Simplified geological map of Greater Antilles showing the main ophiolitic units (purple colour in Figure 1b) (modified from Wadge *et al*. 1984); (b) geological map of eastern Cuba showing the main geological units (modified from Pushcharovsky 1988); (c) geological map of the La Tinta mélange (based on the Geologic Map of the Republic of Cuba, scale 1:100000, sheet 5376, Instituto de Geología y Paleontología, La Habana) showing sample locations: amphibolites (OFT-146a, OFT-146b, OFT-146c-I, OFT-146c-II, OFT-267a, OFT-267d, OFT-267b, OFT-267c, OFT-146 g) and serpentinites (OFT-146e, OFT-146f).

2011a). The associated La Corea and Sierra del Convento serpentinite-matrix subduction mélanges formed shortly after the onset of subduction. These mélanges bear high-pressure/high-temperature (15 kbar; 700–750ºC) amphibolite and anatectic trondhjemite blocks that indicate partial melting of the slab induced by subduction of a hot-young Proto-Caribbean oceanic lithosphere at ca. 120 Ma (Garcia-Casco et al. 2008b; Lázaro *et al*. 2009; Blanco-Quintero *et al*. 2011b. See also Krebs *et al*. 2008; 2011; and Escuder-Viruete *et al*. 2011a; 2013a, 2013b; for similar findings in the Río San Juan mélange, Hispaniola). However, Early Cretaceous boninitic, low-Ti IAT, and FABs have not been described in the eastern Cuba region.

In this article we address the petrology, geochemistry, and geochronology of the La Tinta serpentinite mélange. This mélange has a limited areal exposure close to the southern coast of Cuba, and so far has never been studied in detail. Our research point to this mélange as containing the 'forearc basalts' of the Cuban forearc, and serving these rocks as a proxy to further understand the processes at subduction zone inception. We show that this small geologic body is of importance for setting the plate-tectonic framework of the earliest stages of the Caribbean arc.

2. Geological setting

The Cuban fragment of the Caribbean orogenic belt formed during the Cretaceous–Tertiary convergence and collision of the Caribbean oceanic plate and the North American margin (Pindell *et al*. 1988; Iturralde-Vinent 1998). The Proto-Caribbean (i.e. Atlantic oceanic lithosphere formed during the break-up of Pangea) subducted below the Caribbean plate to form an intraoceanic arc system that finally collided with the Jurassic–Cretaceous passive margin-like terrane of Caribeana (an offshore branch of the Maya block), the continental margin of the Maya block (Guaniguanico terrane) and the Bahamas platform during the latest Cretaceous-Tertiary times (Iturralde-Vinent *et al*. 2008; Garcia-Casco et al. 2008a).

The geology of eastern Cuba includes several tectonic units (Figure 1(b)), namely ophiolitic bodies (i.e. the Mayarí-Cristal and Moa-Baracoa complexes, and the Late Cretaceous metamorphic sole of the latter, the Güira de Jauco Amphibolite Complex, GJAC), Early to Late Cretaceous volcanic arc sequences (i.e. Purial, Quibiján, Santo Domingo, Téneme, and Morel formations), Early Cretaceous high-pressure (HP) subduction mélanges (i.e. Sierra del Convento and La Corea), Late Cretaceous HP metasedimentary rocks (i.e. the Asunción terrane), and Maastrichtian-Danian synorogenic deposits (i.e. La Picota and Mícara formations). The general vergence of thrusting is towards the northeast (Cobiella *et al*. 1984; Núñez-Cambra *et al*. 2004). These directions are related to the final emplacement of the ophiolitic and volcanic arc sheets during the latest Cretaceous to early Danian time (Iturralde-Vinent *et al*. 2006, 2008).

The most significant tectonic units in the area are the Cretaceous volcanic arc and the ophiolitic belts. These constitute, respectively, the structurally deepest and highest pre-Tertiary complexes in the region. The huge Mayarí-Baracoa Ophiolitic Belt (MBOB; Iturralde-Vinent 1996a; Proenza *et al*. 1999; Cobiella-Reguera 2005) consists of two main massifs (Figure 1(b)) likely formed in disparate oceanic environments and emplaced as independent tectonic units: the Mayarí-Cristal Ophiolite Massif, to the West, and the Moa-Baracoa Ophiolite Massif, to the East (Figure 1(b); Proenza *et al*. 1999). A forearc setting for the formation of the Mayarí-Cristal Ophiolite Massif is mainly accepted (Gervilla *et al*. 2005; Proenza *et al*. 2006; Blanco-Quintero *et al*. 2011a), whereas the Moa-Baracoa Ophiolite Massif formed in a backarc to arc environment (Marchesi *et al*. 2006, 2007). Serpentinitic mélanges containing HP blocks occur tectonically below the Mayarí-Cristal Ophiolite Massif (Figure 1(b); the La Corea mélange; Blanco-Quintero *et al*. 2010) and as a body disconnected from the main ophiolitic massifs (Figure 1(b); the Sierra del Convento mélange; Garcia-Casco et al. 2008b). These mélanges contain exotic HP (700–750ºC and ca. 1.5 GPa) blocks of various origins, sizes, and compositions (Ep±Grt-, Pl-lacking amphibolites, tonalitic-trondhjemitic rocks, blueschists, jadeitites) within a serpentinite matrix, which documents the subduction of oceanic and volcanic arc lithosphere since, at least, 120 Ma (Garcia-Casco *et al*. 2006, 2008b, 2009; Lázaro and Garcia-Casco 2008; Lázaro *et al*. 2009, 2011b; Blanco-Quintero et al. 2010; Cárdenas-Párraga *et al*. 2012).

The GJAC forms a thin sheet roughly oriented N–S located at the easternmost edge of the Moa-Baracoa Ophiolite Massif (Figure 1(b,c)). It has been interpreted as the metamorphic sole of the Moa-Baracoa Ophiolite (Lázaro *et al*. 2013, 2015). These amphibolites are of basaltic (MORB-like) protholith formed in a backarc setting (Lázaro *et al*. 2013, 2015). Lázaro *et al*. (2015) suggested that this complex formed during the inception of a new SW-dipping subduction zone in the backarc region of the northern Caribbean arc during the Late Cretaceous (ca. 90–85 Ma) triggered by the main plume pulse of the Colombian–Caribbean Oceanic Plateau. The ophiolitic thrust sheets override the syntectonic foredeep Maastrichtian-Lower Danian olistostromal Mícara (Cobiella 1974) and La Picota (Lewis and Straczek 1955) formations (Figure 1(b); see also Iturralde-Vinent 1976; Cobiella *et al*. 1984; Quintas 1987, 1988; Pushcharovsky 1988). These formations occupy an intermediate discontinuous tectonic position below the ophiolite thrust sheets and the underlying volcanic arc formations (Iturralde-Vinent *et al*. 2006).

The ophiolite sheets, mélanges, and syntectonic sedimentary formations tectonically override the Cretaceous volcanic units (Figure 1; Knipper and Cabrera 1974; Iturralde-Vinent 1976, 1996a, 1996b; Quintas 1988, 1989; Gyarmati and Leyé O'Conor 1990; Torrez and Fonseca 1990; Gyarmati *et al*. 1997; Kerr *et al*. 1999; Iturralde-Vinent *et al*. 2006). These units document axial-arc, backarc, and forearc environments during Early (Aptian–Albian) to Late Cretaceous (mid-Campanian) times (Iturralde-Vinent *et al*. 2006; Proenza *et al*. 2006; Marchesi *et al*. 2007). Fragments of the Campanian and older Cretaceous volcanic arc of the Caribbean (Figure 1; the Purial complex) underwent HP metamorphism (Boiteau *et al*. 1972; Cobiella *et al*. 1977; Somin and Millán 1981; Millán *et al*. 1985; and unpublished data). The age of subduction-related metamorphism is latest Cretaceous (ca. 75–70 Ma; Somin and Millán 1981; Somin *et al*. 1992; Iturralde-Vinent *et al*. 2006).

According to Garcia-Casco et al. (2008a), the HP/low-temperature metasedimentary Asunción terrane is the lowest tectonic unit in the region (Figure 1(c); see Cobiella *et al*. 1984 for a different view). This unit has been related to the Caribeana terrane of the Proto-Caribbean, an intraoceanic sedimentary platform-related domain that subducted during the latest Cretaceous-earliest Tertiary (Garcia-Casco et al. 2008a). A pre-early Danian metamorphic age is suggested by Iturralde-Vinent *et al*. (2006) based on the stratigraphy and in agreement with regional considerations (i.e. like in the Samaná Complex, Hispaniola, Escuder-Viruete *et al*. 2011b).

2.1. The La Tinta mélange

The La Tinta mélange is a small (~ 8–10 km^2) serpentinitic body that crops out to the southeast of the Moa-Baracoa Ophiolite Massif and the metamorphic El Purial volcanic arc complex and to the west of the GJAC (Figure 1(c)). To the south, the body is covered by post-orogenic Tertiary-recent sediments, preventing an estimation of the southern extent of the body. The serpentinite body includes centimetre-to-decimetre-sized blocks of amphibolite (Figure 2), sometimes resembling 'boudins' structures. Our structural recognition indicates that the ultramafic mélange is overridden by the El Purial metavolcanics, which, in turn, are overridden by the nearby Moa-Baracoa Ophiolite. This would make correlation of the La Tinta body with the Moa-Baracoa Ophiolite problematic. On the other hand, the presence of amphibolite blocks within a serpentinitic matrix would allow a tentative correlation with the subduction-related Sierra del Convento and La Corea mélanges. However, the nature and timing of metamorphism of the La Tinta mélange are unknown, and neither tonalitic-trondhjemitic blocks, typical of these mélanges, nor blueschist blocks have been observed. We have studied in detail nine blocks of amphibolite (OFT-146a, OFT-146b, OFT-146c-I, OFT-146c-II, OFT-146 g, OFT-267a, OFT-267d, OFT-267b, and OFT-267c) and two samples of enclosing serpentinites (OFT-146e and OFT-146f).

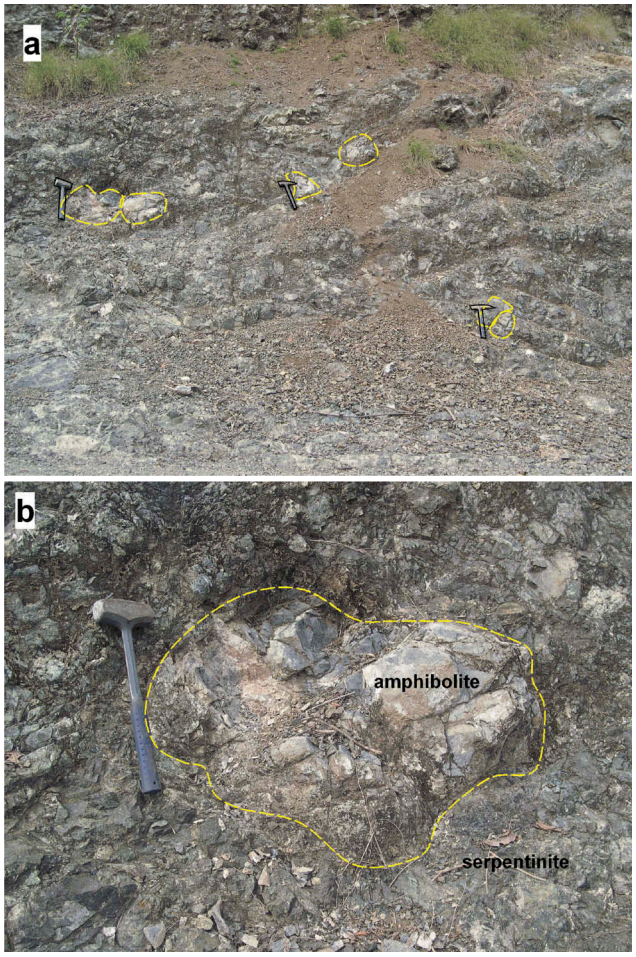

Figure 2. (a) Amphibolite blocks within serpentinite; (b) detail of block of amphibolite within serpentinite.

3. Analytical Methods

Whole-rock geochemistry and mineral chemistry analyses were performed at the Scientific Analytical Centre (CIC – Centro de Instrumentación Científica), University of Granada. Mineral compositions were obtained by Wavelength Dispersive Spectroscopy (WDS) with a CAMECA SX-100 microprobe, operated at 15 kV and 15 nA, with a beam size of 5 μm and the standards used for element calibrations were: albite (Na), quartz (Si), periclase (Mg), sanidine (K), rutile (Ti), haematite (Fe), diopside (Ca), vanadinite (Cl), barite (Ba), fluorite (F), chromite (Cr), Al_2O_3 (Al), $MnTiO_3$ (Mn), and NiO (Ni). Detection limit is in the range 0.005–0.010 oxide wt.%, accuracy in the range 1–3 relative per cent, and precision in the range ~ 1 relative per

cent. Amphibole compositions were normalized following the procedures of Leake *et al*. (1997), and Fe^{3+} was estimated after the method of Schumacher (in Leake *et al*. 1997). Epidote and feldspar were normalized to 12.5 and 8 oxygens, respectively, and $Fe_{total} = Fe^{3+}$. Clinopyroxene was normalized to four cations and six oxygens, with Fe^{3+} estimated by stoichiometry (Morimoto *et al*. 1988). Olivine and spinel were normalized to three cations and four oxygens, and Fe^{3+} was estimated by stoichiometry. Chlorite and serpentine were normalized to 28 and 14 oxygens, respectively, and $Fe_{total} = Fe^{2+}$. Atoms per formula unit are abbreviated apfu. The Mg number of minerals and rocks (Mg#) represents the atomic $Mg/(Mg+Fe^{2+})$ and $Mg*100/(Mg + Fe_{total})$, respectively. Mineral and end-member abbreviations are after Whitney and Evans (2010). The analyses are presented in Supplementary Tables 1–5 (see http://dx.doi.org/10.1080/00206814.2015.1118647 for supplementary tables).

Whole-rock major-element determinations were carried out by X-ray fluorescence spectrometry (XRF) on glass beads using a Philips PV1404 spectrometer at the University of Granada. Precision was better than ±1.5% for a concentration of 10 wt.%. Zr was determined by XRF on pressed powder pellets, with a precision better than ±4% at 100 ppm concentration. The analyses were recalculated to an anhydrous 100 wt.% basis, and these data are used in the figures. Other trace elements were analysed by ICP-MS (University of Granada). Procedural blanks and international standards PMS, WSE, UBN, BEN, BR, and AGV (Govindaraju 1994) were run as unknowns during analytical sessions. Precision was better than ±2% and ±5% for analyte concentrations of 50 and 5 ppm, respectively. The analyses are presented in Supplementary Table 6.

Preparation of mineral samples before and after irradiation for $^{40}Ar/^{39}Ar$ analyses was carried out at the ARGONAUT Laboratory of the Geology Division at the University of Salzburg (Austria). Hornblende concentrates were prepared by crushing, sieving, flotation, and handpicking of grains in the size ranges 250–200 and 250–125 µm. For isotopic measurements, 10–20 grains per sample were selected, and the mineral concentrates were packed in aluminium foil and loaded in quartz vials. To calculate the J-values, flux monitors were placed between each four and five unknown samples, which yielded a distance of ~5 mm between adjacent flux monitors. The sealed quartz vials were irradiated in the MTA KFKI reactor (Debrecen, Hungary) for 16 h. Correction factors for interfering isotopes were calculated from 10 analyses of two Ca-glass samples and 22 analyses of two pure K-glass samples, and are: $^{36}Ar/^{37}Ar(Ca) = 0.00026025$, $^{39}Ar/^{37}Ar(Ca) = 0.00065014$, and $^{40}Ar/^{39}Ar(K) = 0.015466$. Variations in the flux of neutrons were monitored with a DRA1 sanidine standard for which a $^{40}Ar/^{39}Ar$ plateau age of 25.03 ± 0.05 Ma has been reported by Wijbrans *et al*. (1995). After irradiation, the minerals were unpacked from the quartz vials and aluminium-foil packets and handpicked into 1 mm-diameter holes within one-way Al-sample holders.

$^{40}Ar/^{39}Ar$ analyses were carried out using a UHV Ar-extraction line equipped with a combined MERCHANTEK™ UV/ IR laser ablation facility and a VG-ISOTECH™ NG3600 mass spectrometer and follow the methods described in Handler *et al*. (2004). Stepwise heating analyses of samples were performed using a defocused (~1.5 mm diameter) 25 W CO2-IR laser operating in Tem00 mode at wavelengths between 10.57 and 10.63 lm. The laser is controlled from a PC, and the position of the laser within the sample is monitored through a double-vacuum window on the sample chamber via a video camera in the optical axis of the laser beam on the computer screen. Gas clean-up was performed using one hot and one cold Zr-Al SAES getter. Gas admittance and pumping of the mass spectrometer and the Ar-extraction line are computer-controlled using pneumatic valves. The NG3600 is an 18 cm-radius 60° extended geometry instrument, equipped with a bright Nier-type source operated at 4.5 kV. Measurements were performed on an axial electron multiplier in static mode on a single-collector instrument. Peak jumping and stability of the magnet are controlled by a Hall probe. For each increment, the intensities of ^{36}Ar, ^{37}Ar, ^{38}Ar, ^{39}Ar, and ^{40}Ar were measured, and the baseline readings on mass 35.5 are automatically subtracted. Intensities of the peaks were back-extrapolated over 16 measured intensities to the time of gas admittance either by a straight line or by a curved fit, depending on the shape of the curve. Fit by a straight line is typical for low intensities and curved fit for high intensities. Intensities were corrected for system blanks, background, post-irradiation decay of ^{37}Ar, and interfering isotopes. Isotopic ratios, ages, and errors for individual steps were calculated following suggestions by McDougall and Harrison (1999) and using decay constants recommended by Steiger and Jäger (1977). Plateau and integrated ages were calculated using the ISOPLOT/ EX 3.00 software (Ludwig 2001). Time-scale calibration follows Gradstein and Ogg (2005). The analyses are presented in Supplementary Table 7.

4. Petrography and mineral composition

4.1. Petrography

Two types of amphibolite rocks can be differentiated: (i) clinopyroxene-bearing amphibolite (OFT-146 g, OFT-267a) and (ii) clinopyroxene-lacking amphibolite

(OFT-146a, OFT-146b, OFT-146c-I, OFT-146c-II, OFT-267d, OFT-267b, OFT-267c). The clinopyroxene-bearing amphibolites are massive, medium-grained (~1 mm), and locally show granoblastic texture and the retrograde transformation of diopsidic clinopyroxene into amphibole (Figures 3(a,b) and 4(a,c)). No fabric elements with a preferred orientation are observed in the samples. The peak mineral assemblages of these rocks all contain calcic amphibole + plagioclase + calcic clinopyroxene. Minor apatite + ilmenite + magnetite + haematite occur as accessory phases. The rocks are partially retrograded to tremolite-actinolite amphibole, prehnite, and chlorite. Prehnite appears mostly in late retrogression patches associated with chlorite. The blocks of Cpx-lacking amphibolite, on the other hand, are similarly massive, fine to medium grained, but, notably, show a relict magmatic ophitic texture best identified by pseudomorphs of plagioclase. These pseudomorphs are largely saussuritized (Figures 3(d) and 4(b)), showing metadolerite rock protholith textures (Figure 3(c,d)). The peak mineral assemblages of these rocks are also homogeneous and consist of calcic amphibole + plagioclase.

The ultramafic rocks (OFT-146e, OFT-146f) are highly serpentinized (more than 96 mode %) and only a few grains of relict olivine and chromian spinel (~4 mode %) appear surrounded by the serpentine mesh. The serpentine minerals are fibrous and locally show hourglass texture, indicating low-temperature polymorph lizardite. Relic olivine occurs as colourless clear grains of

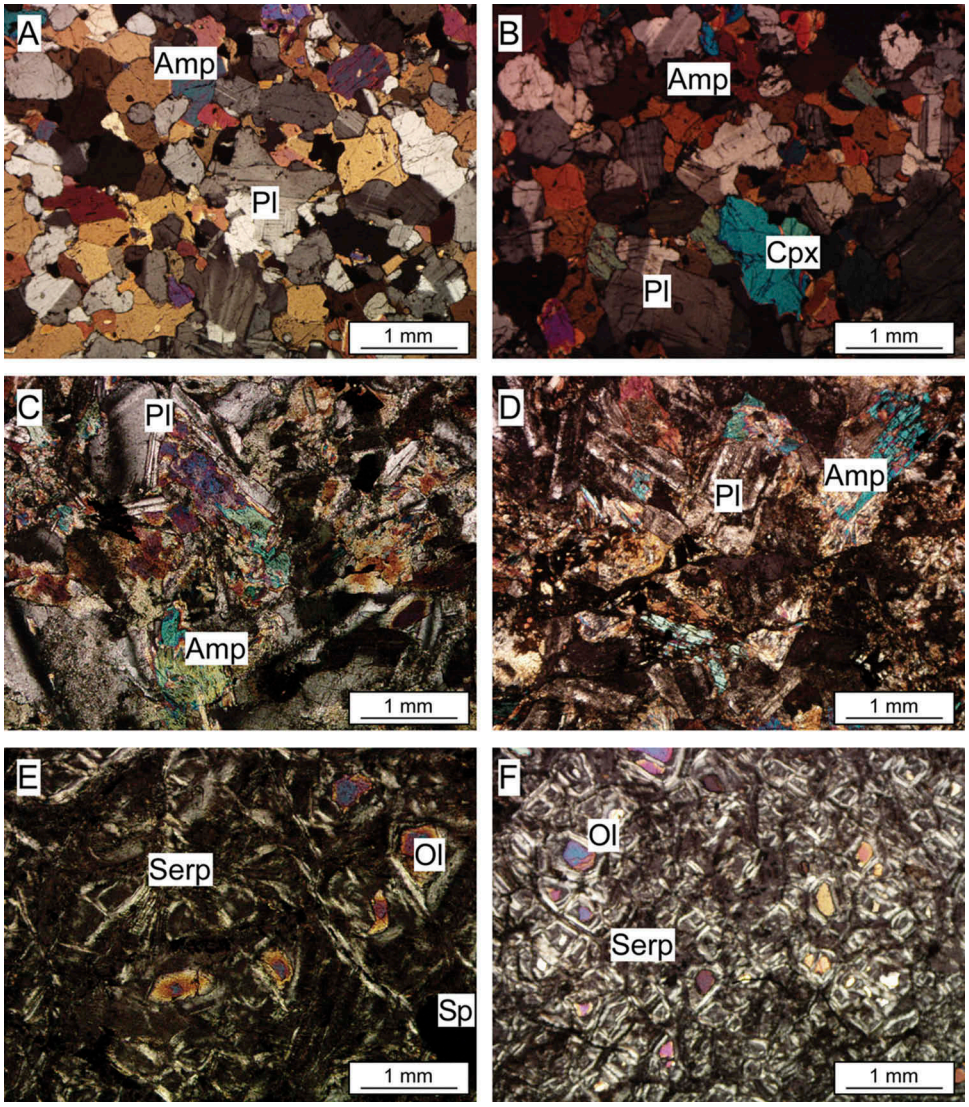

Figure 3. Optical images of (a) and (b) clinopyroxene-bearing amphibolite with granoblastic texture; (c) and (d) clinopyroxene-lacking amphibolite with saussuritized plagioclase and amphibole with ophitic texture; (e) and (f) serpentinized ultramafic rocks showing olivine and hourglass texture of serpentine-group minerals (likely, lizardite) indicating relatively low temperature during serpentinization.

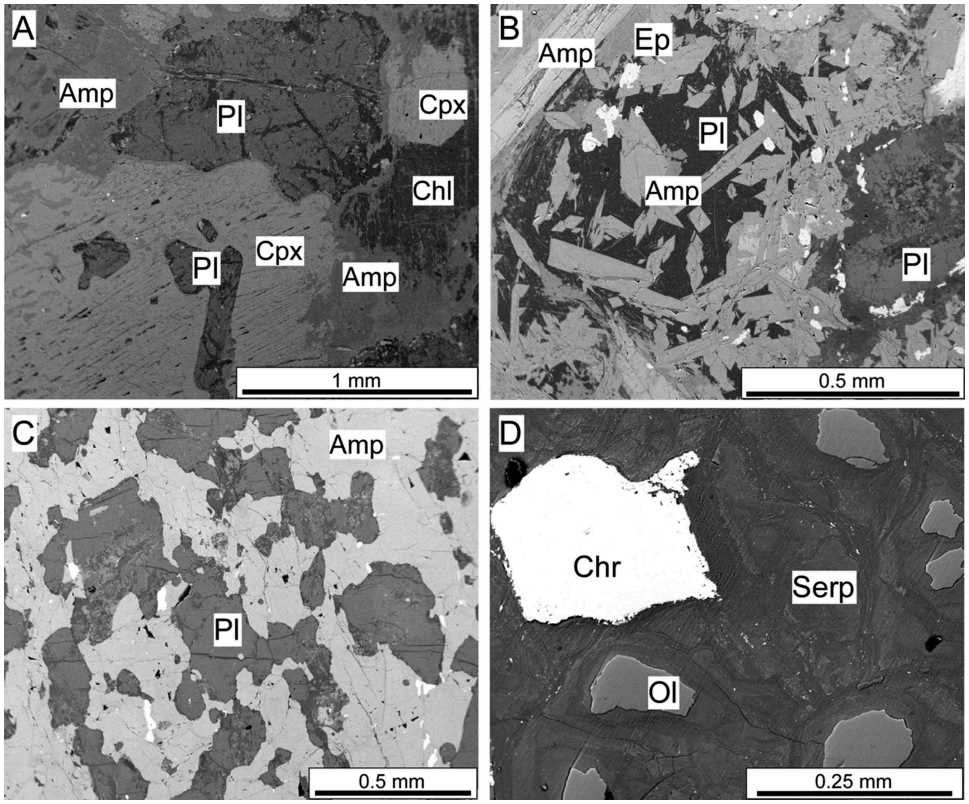

Figure 4. BSE images: (a) amphibole surrounding pyroxene and plagioclase, and chlorite after amphibole in the clinopyroxene-bearing amphibolite; (b) newly formed amphibole and altered plagioclase grains; (c) amphibole and newly formed plagioclase; (d) concentric alteration of olivine grains to serpentine and a chromite grain from serpentinite.

100–200 μm in length (Figure 3(e,f)). Serpentinized grains are normally encircled by fibrous serpentine rims (Figure 4(d)). The pseudomorphs are anhedral, showing wavy/radial extinction. Scarce chromian spinel grains occur as fresh small crystals having a uniform brown-dark colour. In some cases the crystals (up to 1 mm in diameter) are broken and the cracks are occupied by serpentine.

4.2. Mineral chemistry

4.2.1. Amphibole

The amphiboles are calcic in all rocks types, having CaB = 1.51–1.96 apfu content. The clinopyroxene-bearing amphibolites have tschermakite-magnesiohornblende-actinolite-tremolite (Si = 6.39–7.82, Al_{total} = 0.23–2.14, Na_{total} = 0.05–0.58, Na(B) = 0.01–0.19 apfu and (Na+K)A = 0.03–0.48 apfu) compositions (Supplementary Table 1; Figure 5(a)). The Mg# of amphibole is varied as a function of amphibole composition (Mg# generally increases from tschermakite to actinolite/tremolite) and of whole-rock compositions (Figure 5(a,c)). The variations in Ti are appreciable, with higher contents in the Si-poor grains (i.e. tschermakite compositions), up to ca. 0.25 apfu; Figure 5(b,d). In the Cpx-lacking amphibolite samples, amphibole has tschermakite-magnesiohornblende-actinolite compositions (Supplementary Table 1, Figure 5(e,f)), with Si = 6.41–7.96 apfu, Al_{total} = 0.04–1.88 apfu, Na_{total} = 0.03–0.57, Na(B) is 0.02–0.24 apfu, and (K+Na)A = 0.02–0.49 apfu.

4.2.2. Plagioclase

The clinopyroxene-bearing amphibolites have unaltered plagioclase grains, with small chemical variation per sample, having labradorite compositions (Xan = 0.50–0.58) in sample OFT-146 g (Supplementary Table 2; Figure 6(a)). Plagioclase in Cpx-lacking amphibolites having a pseudomorphic doleritic texture displays wider compositional variations, from labradorite to albite (Xan = 0.64–0.01), reflecting compositions of relict plagioclase from the protholith (labradorite) and newly formed metamorphic plagioclase (andesine-albite; Supplementary Table 2; Figure 6(b)). All compositions are very low in K (< 0.04 apfu).

4.2.3. Pyroxene

Clinopyroxene is augite-diopside (Supplementary Table 3), with Wo = 43.61–47.29, En = 36.72–37.82, Fs = 15.60–19.25, Mg# = 0.66–0.73, and low Al contents (< 0.05 apfu). The Fe^{3+} (<0.04 apfu) and Na (< 0.03

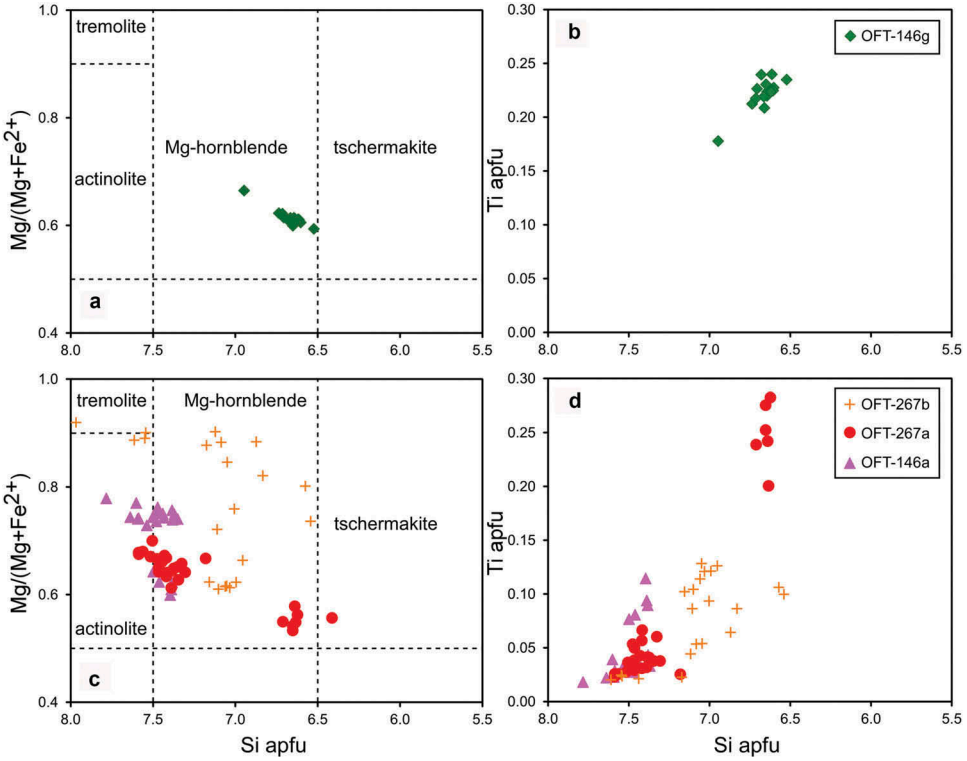

Figure 5. Composition of calcic amphibole: (a), (c) Si *versus* Mg/(Mg+Fe^{2+}) and (b), (d) Ti *versus* Si.

apfu) are very low, suggesting the low pressure of crystallization.

4.2.4. Chlorite

Chlorite in the clinopyroxene-bearing amphibolite has Si = 5.73–6.17, Mg = 7.37–9.03, and Fe = 0.89–1.82, with low Mn and Ni (<0.04 apfu) contents (Supplementary Table 4). Chlorite is clinochlore according to the Si and Mg# = 0.81–0.91 contents (Hey 1954). Chlorites in Cpx-lacking amphibolites have similar Si (5.71–6.45 apfu) but lower Mg (5.50–6.75 apfu) and higher Fe (2.64–3.16 apfu), with low Mn (<0.04 apfu) content (Supplementary Table 4). These compositions are classified as pycnochlorite according to the Si contents and Mg# = 0.64–0.72 (Hey 1954).

4.2.5. Other minerals

Epidote group minerals have variable Fe^{3+} contents (0.01–0.33 apfu, Supplementary Table 4), but show no clear zoning trend. Prehnite has low Fe^{3+} (<0.03 apfu, Supplementary Table 4). Ilmenite, magnetite, and haematite appear in all types of amphibolites, showing very low Mn <0.07 apfu and Mg <0.05 apfu contents.

4.2.6. Olivine

Relict mantle olivine compositions in serpentinites range from Fo91 to Fo93. Nickel contents vary between 0.31 and 0.43 NiO wt.%, and Mn contents reach up to 0.15 MnO wt.%, indicating compositions typical of mantle olivine. They have negligible Al_2O_3, CaO, and TiO_2 contents, less than 0.04 wt.% (Supplementary Table 5).

4.2.7. Serpentine

Serpentine minerals have Si = 3.42–3.99, Mg = 5.41–6.37, Fe = 0.19–0.73, Cr < 0.15, and Ni < 0.04 apfu contents (Supplementary Table 5). In the ternary diagram molar % Mg-Si-Fe (Figure 7) all these values show lizardite and minor chrysotile composition, corresponding to the textures and the relatively high Al contents of up to 0.40 apfu.

4.2.8. Chromian spinel

The composition of relict spinel in serpentinites is magnesiochromite, with Cr# in the range of 0.57–0.60, Mg# in the range 0.50–0.58 (Figure 8, Supplementary Table 5), and low TiO_2 (<0.17 wt.%). The grains are usually not affected by alteration as indicated by the low Fe^{3+} content (<0.10 apfu).

5. Whole-rock composition

The whole-rock major element compositions of the amphibolites span a relatively narrow range, with SiO_2 = 47–52 wt.%, Al_2O_3 = 15–17 wt.%, CaO = 8–15 wt.%, and MgO = 6–8 wt.% (Supplementary Table 6) and variable Na_2O concentrations (from 0.04

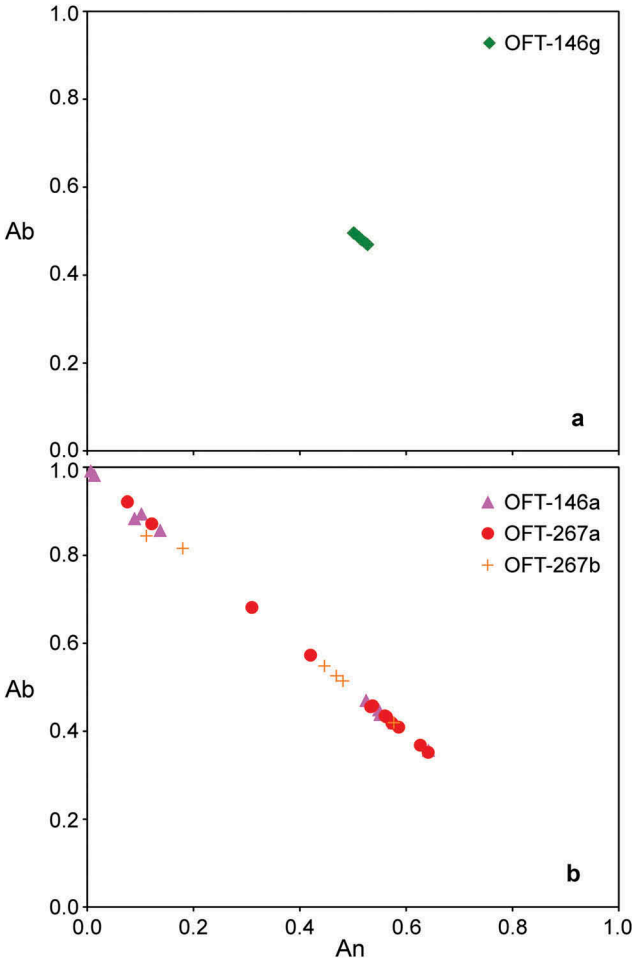

Figure 6. An-Ab plagioclase compositions of the (a) the clinopyroxene-bearing amphibolites and (b) the clinopyroxene-lacking amphibolites.

to 0.9 wt.%). The use of major elements for characterizing the protholith of metamorphic rocks is risky because of their mobile character during prograde and retrograde metamorphism. Therefore, we used elements that generally are immobile during metamorphism (Ti, Al, Mn, and P; Pearce 1976; Rollinson 1983).

In the Nb/Y *versus* Zr/TiO_2 immobile trace element plot of Figure 9(a), the amphibolites are sub-alkaline and show basaltic compositions. The TiO_2-MnO-P_2O_5 ratios and the variation of total Fe as FeO/MgO = 0.8–1.9 of samples indicate a tholeiitic signature. The chondrite-normalized rare earth patterns are homogeneous with a typical N-MORB pattern showing distinctive LREE depletion (Figure 10(a,c)), with La/Yb ratios between 0.4 and 0.9. However, their primitive mantle-normalized element patterns show spikes with slight Nb and Th depletion (Figure 10(b,d)).

All samples of amphibolite are enriched in Ba, Rb, and K as a likely consequence of hydration during metamorphism (Figure 10(b)). Similar enrichments observed in boninites from the Izu-Bonin-Mariana (IBM) forearc are interpreted as a primary characteristic rather than secondary alteration fluids (Reagan *et al.* 2010), whereas low-Ti depleted (boninites) and high-Ti tholeiites from the Nuvvuagittuq belt are considered metasomatic after the infiltration of hydrothermal fluids (Turner *et al.* 2014).

Serpentinite samples have refractory bulk-rock compositions with low contents of immobile incompatible elements, such as Al, Ti, and V (Supplementary Table 6). The concentration of immobile refractory elements, such as Ni (>2000 ppm) and Cr (>1200 ppm), is high. Bulk-rock Mg# is high, 90.5 and 91.1, and CaO is very low (less than 0.5 wt.%) for both samples. Although calcium is mobile during seafloor hydrothermal activity and/or metamorphic hydration + recrystallization, the consistency with the low Al_2O_3 and high Mg# and Cr contents suggests that the low CaO content is a primary feature of the studied samples. In the Al_2O_3/SiO_2 *versus*

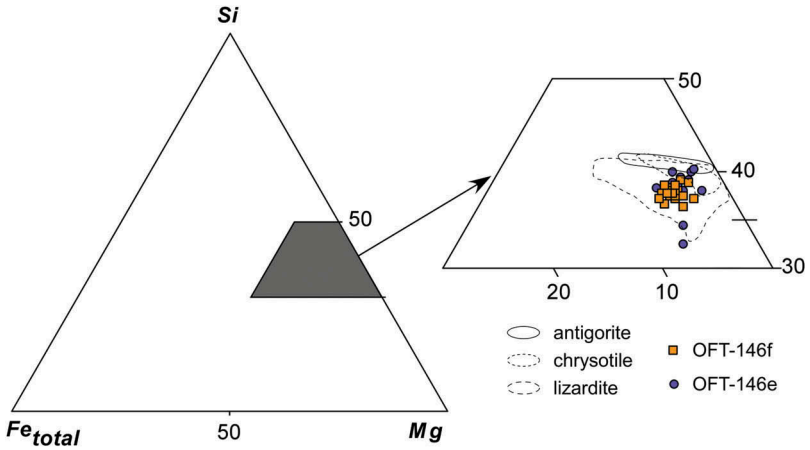

Figure 7. Ternary atomic Mg-Si-Fe diagram showing the chemical variability of serpentine minerals from serpentinites. The fields of lizardite, chrysotile, and antigorite compiled by D'Antonio and Kristensen (2004).

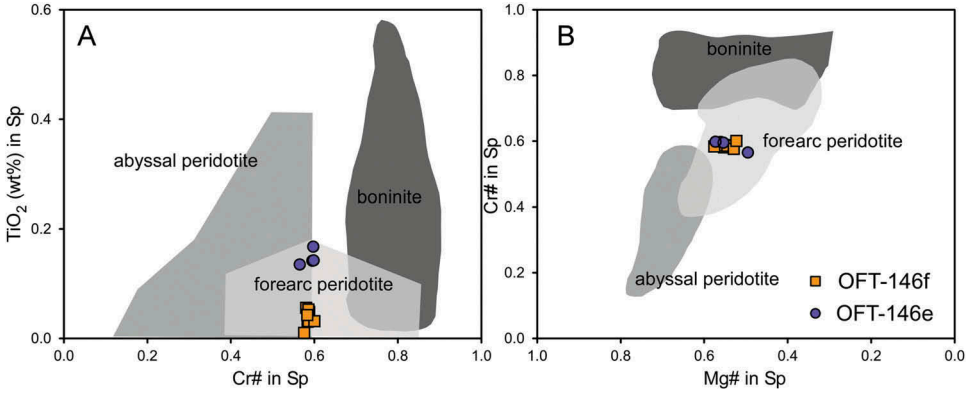

Figure 8. Compositional variations of spinels from ultramafic rocks: (a) Cr# *versus* TiO_2 (wt.%); and (b) Mg# *versus* Cr# . The abyssal, forearc, and boninite fields are after Uysal *et al*. (2007).

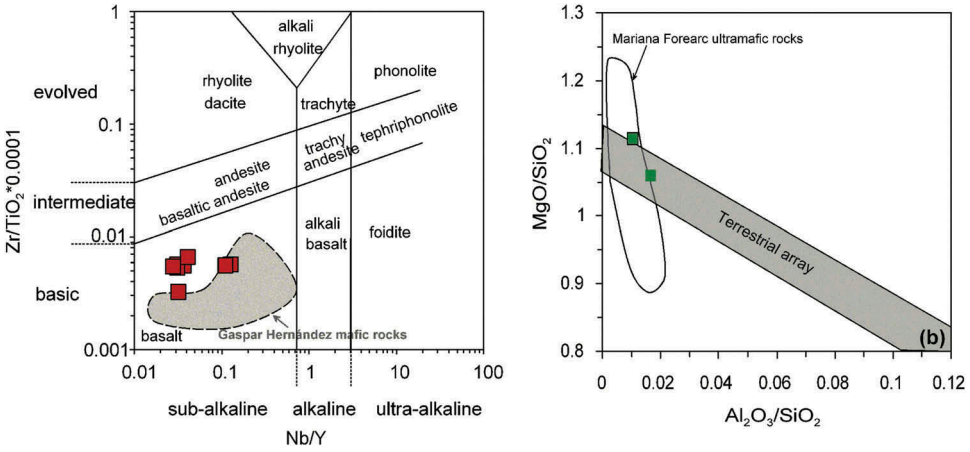

Figure 9. (a) Nb/Y *versus* Zr/TiO_2 diagram (Winchester and Floyd 1977) for amphibolites from the La Tinta mélange. (b) Bulk rock Al_2O_3/SiO_2 *versus* MgO/SiO_2 for La Tinta meta-ultramafic rocks. The terrestrial array is from Hart and Zindler (1986), and, for comparison, the Gaspar Hernandez mafic rocks (Hispaniola; Escuder-Viruete *et al*. 2011a) and the Mariana forearc (compiled by Hattori and Guillot 2007).

MgO/SiO_2 diagram (Figure 9(b)), serpentinites plot in the left region of the terrestrial array (Hart and Zindler 1986), where the field of forearc mantle peridotites, as the IBM ultramafic rocks, is located.

6. P-T conditions and age of metamorphism

6.1. P-T conditions

An isochemical P-T projection (pseudosection) was calculated for a representative bulk-rock composition of the studied rocks having a mineral assemblage with the lowest thermodynamic variance (OFT-146 g; Supplementary Table 6). The pseudosection was calculated in the NCFMASHTO system using the Perple_X software (Connolly 2005). A fluid phase, assumed to be pure H_2O, was considered in excess. Components K_2O and MnO are neglected because they have very low concentration in the rocks and are diluted in the coexisting phases. The amount of ferric iron was set at 10 mole % of total iron, appropriate for basic rocks. The solution models used for amphibole, plagioclase, clinopyroxene, orthopyroxene, chlorite, and epidote are those of Dale *et al*. (2005), Newton *et al*. (1980), Green *et al*. (2007), Holland and Powell (1996), Holland *et al*. (1998), and Holland and Powell (1998), respectively, and an ideal model for ilmenite-haematite.

The pseudosection (Figure 11(a)) shows a large field in the lower right part of the P-T window, with the association Hbl+Cpx+Pl+Ilm+Mag, consistent with the observed peak mineral assemblages in sample OFT-146 g. To further constrain the P-T conditions, mineral composition isopleths for plagioclase (Xan) and diopsidic pyroxene (Mg#) were determined (Figure 11(b)). The distribution of isopleths confirms the field and fixes the

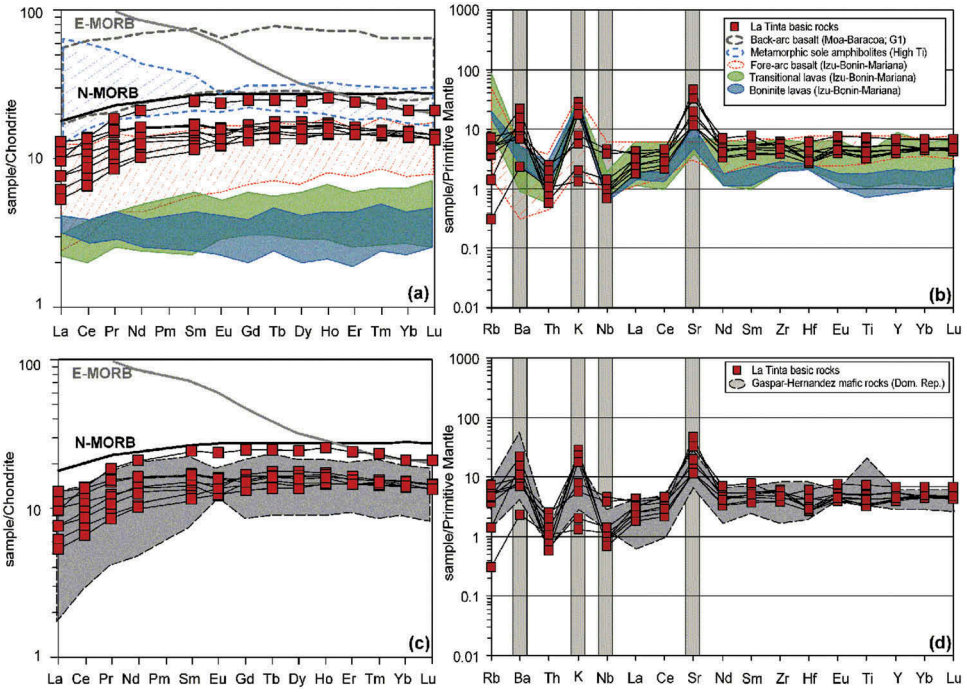

Figure 10. (a, c) Chondrite (CI)-normalized (McDonough and Sun 1995) REE abundances and (b, d) primitive mantle-normalized (Sun and McDonough 1989) trace-element concentrations of amphibolites from La Tinta mélange. For reference, normal and enriched mid-ocean ridge basalts (N-MORB and E-MORB, respectively) after Sun and McDonough (1989) are plotted. Also, (a) the backarc basalts of the Moa-Baracoa Ophiolite Massif (Marchesi *et al*. 2007) and the amphibolites from the Moa-Baracoa metamorphic sole (Güira de Jauco Amphibolite Complex, Lázaro *et al*. 2013); (a, b) the forearc basalts, transitional lavas, and boninite lavas from Izu-Bonin-Mariana (Reagan *et al*. 2010; Stern *et al*. 2012) are also plotted for comparison. In (c, d) mafic rocks from Gaspar Hernandez complex (Hispaniola; Escuder-Viruete *et al*. 2011a) are also plotted.

conditions to ca. 3.8 kbar and 720ºC. These conditions indicate high temperature at 12–13 km depth (i.e. in the lithospheric mantle).

These low-P conditions of metamorphism can be extended to all Cpx-bearing rocks because (i) they have similar peak (Pl+Hbl+Cpx) assemblages and (ii) all rocks are barely foliated, indicating static tectonic regimen during metamorphism. Furthermore, the close spatial relationship of all types of amphibolite in the same serpentinitic matrix suggests that similar low-P conditions at somewhat lower-medium T attended metamorphism of the Cpx-lacking blocks of amphibolite. We hence conclude that the blocks represent disrupted dikes/sills of basaltic rocks emplaced in ultramafic rocks of the upper part of an oceanic lithosphere mantle (~12 km).

6.2. Age of metamorphism

The results of the $^{40}Ar/^{39}Ar$ incremental heating analyses and a summary of age and isochron calculation results are presented in Supplementary Table 7 and are graphically shown in Figure 12. Hornblende of sample OFT-146 g yields a staircase pattern with ages of 78–90 Ma in steps 2–4 and a well-defined plateau age of 123.2 ± 2.2 Ma (2σ) based on 89.0% of the released ^{39}Ar (steps 5–8; Supplementary Table 7; Figure 12). The isochron correlation age (ICA) of all steps of hornblende, equally weighted according to model 2 in the software ISOPLOT/ EX (Ludwig 2001), is 119.1 ± 3.1 Ma, with a $^{40}Ar/^{36}Ar$ intercept at 276.4 ± 2.9 (Figure 12), which is close to the atmospheric value of 295.5 and mean square weighted deviation = 1.5 (Figure 12). Although the plateau age is dominated by step nº 8, which contributes 68.0% of ^{39}Ar released and gives an age of 121.6 ± 1.1, it is within error of the ICA. So, the plateau and ICAs are also similar within error. Therefore, we suggest that the plateau age is geologically significant and dates cooling through 500–550°C after peak conditions of metamorphism according to the experimentally determined Ar retention temperature of hornblende (Harrison 1981; McDougall and Harrison 1999). The younger ages of 78–90 Ma of steps 2–4, included in the isochron age of 119.1 ± 3.1 Ma, have a lower K/Ca ratio (Supplementary Table 7) due to a distinct compositional zoning and bear a low component of $^{40}Ar^*$, and are, therefore, likely geologically meaningless.

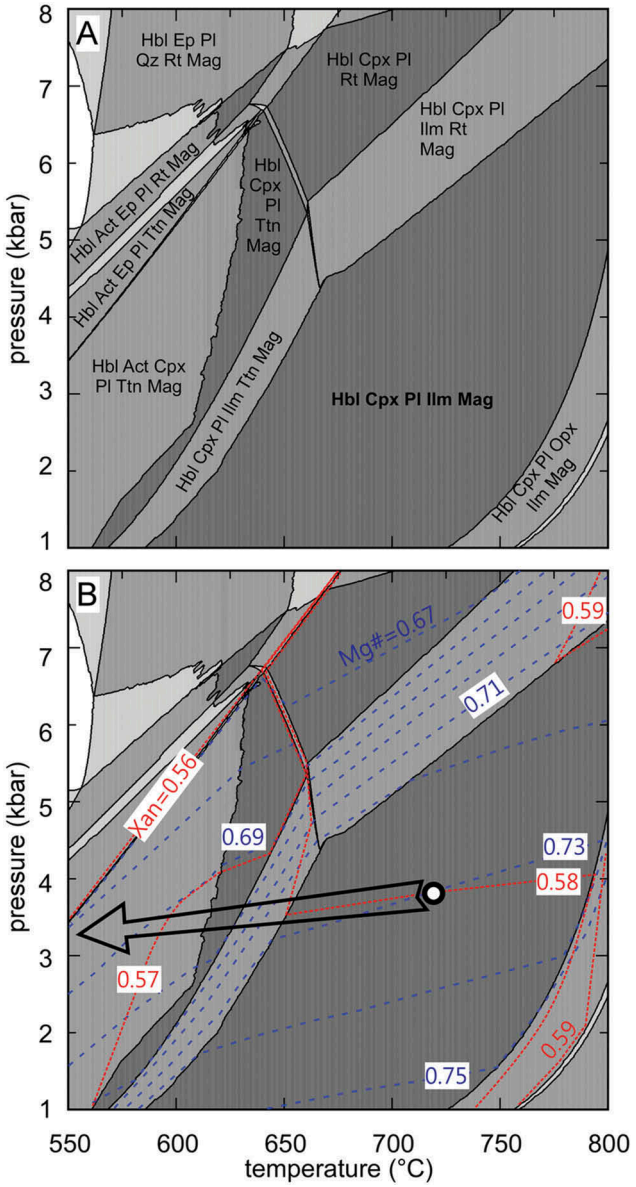

Figure 11. (a) Isochemical P-T equilibrium phase diagram for sample OFT-146 g calculated with Perple_X. Mineral abbreviations after Whitney and Evans (2010). (b) Isopleths for anorthite proportion in the plagioclase (dotted lines) and Mg# in the clinopyroxene (dashed lines) are indicated. The P-T conditions and the cooling trajectory are drawn.

7. Discussion

7.1. Origin of the mafic and ultramafic rocks from the La Tinta mélange.

Stern (2004), Reagan *et al*. (2010), and Stern *et al*. (2012) proposed that basalts of a proto-forearc crust form at the initial stage of a subduction zone, when sinking of the slab and rapid trench rollback provoke the upwelling of the fertile asthenosphere that produces melts with a minor amount of subduction component, in contrast to younger forearc lavas. The amphibolites from the La Tinta mélange have MORB-like signatures similar to FAB (or BABB), lacking a significant subduction-related component. The HFSE (i.e. Zr, Hf, Nb, Ta, Ti) *versus* REE ratios are similar to MORB (Figure 13). The La Tinta amphibolites are slightly depleted in Nb and Th (Figures 10 and 14), whereas the observed enrichment in Sr, Ba, and K is, at least to a great extent, related to hydration during metamorphic transformation (Figure 10(b,d)). The data plotted in the discrimination Al_2O_3/TiO_2 *versus* TiO_2 diagram of Hickey and Frey (1982) allows suggesting that most samples clearly preserve a MORB-like affinity (Figure 13(a)). The TiO_2 contents (ca. 1 wt.%) and FeO_{total}/MgO ratios of the amphibolites are lower than those of normal MORB and similar to the IBM FAB (Figure 13(b)). Moreover, the HFSE and REE *versus* V ratios (e.g. TiO_2/V and Yb/V; Figure 13(c,d)) are slightly lower than in MORB and most backarc basin lavas (e.g. the Moa-Baracoa ophiolite-related volcanics; Marchesi *et al*. 2007). In fact, the chemical composition of the amphibolites is similar to that of subduction-related basalts of the IBM FAB (Stern *et al*. 2012). In the Nb/Yb *versus* Th/Yb diagram, the La Tinta amphibolites plot in the overlapping fields of N-MORB and along the unmodified 'mantle array' and of the FABs, whereas (younger) forearc subduction-influenced lavas trend towards Th/Yb ratios typical of island arc lavas (Figure 14).

A forearc position for the emplacement of these rocks is also suggested by the Ti, Cr#, and Mg# contents of magnesiochromite from the enclosing serpentinites (Figure 8(a,b)). Whereas tectonic setting based in the Cr# *versus* TiO_2 in the spinel diagram is ambiguous (Figure 8(a)), a forearc position is confirmed by the Mg# *versus* Cr# in the spinel diagram (Figure 8(b)). The moderate Cr# of spinel and the Mg# of olivine suggest ca. 30% melting of the ultramafic protoliths of the serpentinites, consistent with a forearc setting (Figure 15; Arai 1992).

The mineral and bulk rock compositions of the studied samples exhibit that the ultramafic and associated amphibolites rocks formed in a forearc environment of the Cretaceous Caribbean arc. The geochemical characteristics of the La Tinta amphibolites are similar to those of the IBM FABs and the Hispaniola Gaspar Hernandez mafic igneous rocks (Figures 10–15), the latter of Early Cretaceous age. Hence, the pre-123.2 ± 2.2 Ma magmatic protoliths of the La Tinta amphibolites represent fragments of the Cretaceous proto-forearc spreading lithosphere.

7.2. Metamorphic evolution and age significance at forearc position in the supra-subduction zone setting

The mineral assemblages of the La Tinta amphibolite blocks (plagioclase + hornblende ± diopside) and the

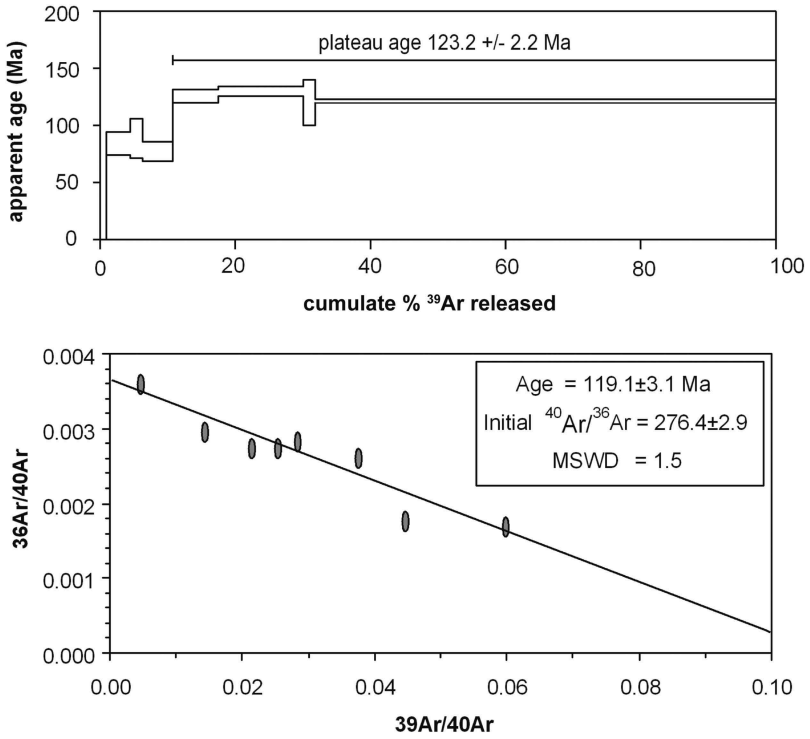

Figure 12. Incremental step heating analyses of amphibole from clinopyroxene-bearing amphibolite sample OFT-146 g. The heights of the rectangles and all errors represent ±1σ uncertainty.

P-T conditions determined indicate low-pressure/high-temperature metamorphism (Figure 11). These low-pressure conditions are also suggested by the low contents of Na(B) in the amphibole compositions and the absence of garnet and/or epidote in the peak metamorphic assemblage of all samples. The absence of fabrics or textures produced by strain (Figures 3 and 4) and retrograde growth zoning of amphibole indicate cooling during static metamorphic recrystallization. These processes are best explained in the context of ocean floor-like metamorphism at shallow mantle depths (at ~12 km depth). Extension of the forearc lithosphere and the associated infiltration of fluids (likely from the sea) shortly after the onset of subduction allowed the development of metamorphism in a cooling forearc and mélange formation as a consequence of serpentinization and fragmentation of the dikes/sills. Hence, this mélange differs from the nearby HP Sierra del Convento and La Corea mélanges formed in the subduction channel after accretion of fragments of the subducted Proto-Caribbean slab to the mantle wedge (Caribbean Plate) (Garcia-Casco et al. 2008b; Lázaro *et al*. 2009, 2011b; Blanco-Quintero *et al*. 2010). The textures of the amphibolites, resembling metadolerite igneous textures, suggest a hypoabissal origin, dikes or sills, for the samples. The metamorphosed dikes would break, resulting in blocks incorporated in the serpentinitic low-pressure-blocks mélange, in a relatively late stage of the tectonic evolution of the region.

The boninitic rocks and low-Ti IAT of Hispaniola are Early Cretaceous in age (Lewis et al. 2002; Kesler *et al*. 2005; Escuder-Viruete *et al*. 2010, 2011a, 2014; Monthel 2010). A sample of microgabbro sill from Gaspar Hernandez serpentinized peridotite-tectonite yielded a U–Pb zircon concordia age of 136.4 ± 0.34 Ma (Escuder-Viruete *et al*. 2011a). This age was interpreted as the crystallization age of the microgabbro in a MORB environment. However, it may suggest that the Gaspar Hernandez peridotite and associated mafic rocks formed in the forearc environment, in harmony with its reinterpreted FAB composition. This age is in agreement with the $^{40}Ar/^{39}Ar$ amphibole cooling age of sample OFT-146 g here provided, which indicates a pre-123 ± 2.2 Ma age of the FAB protolith. The slightly younger development of the boninitic, low-Ti IAT, and normal IAT volcanic sequences of the Maimón, Amina, and Los Ranchos formations took place at 118–110 Ma (Kesler *et al*. 2005; Escuder-Viruete *et al*. 2006), indicating that magmatism likely resumed in the forearc region and concentrated in the young arc region by 120 Ma.

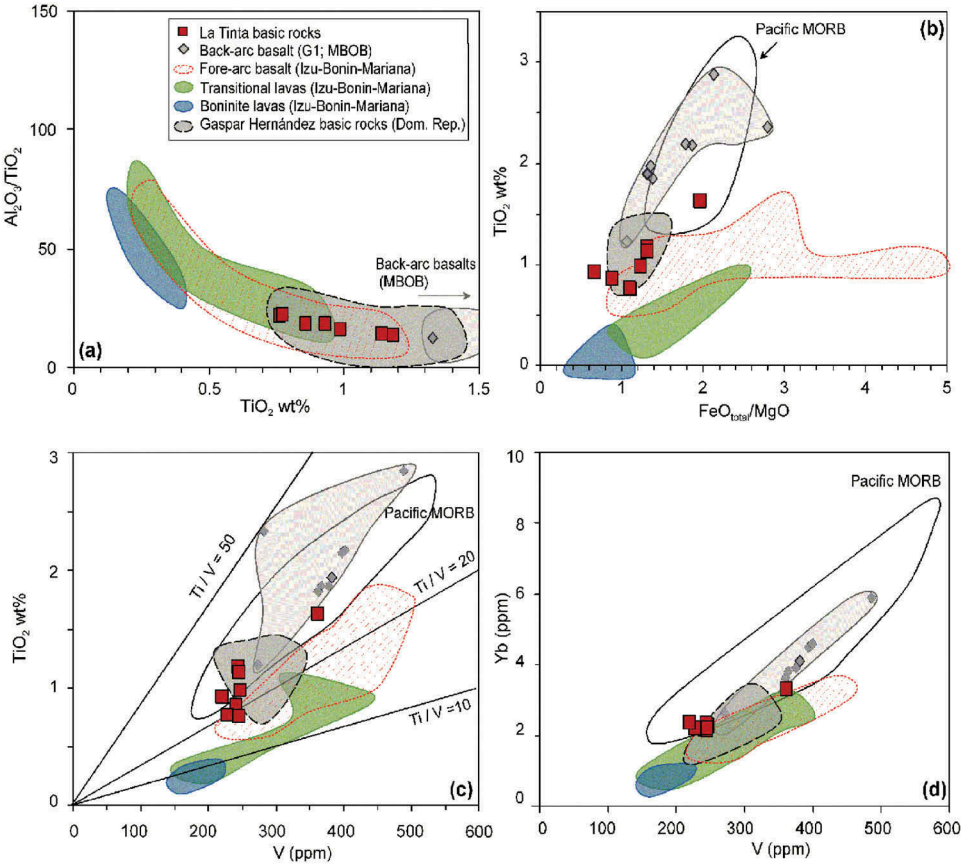

Figure 13. Chemical variation of the La Tinta amphibolites in (a) Al_2O_3/TiO_2 *versus* TiO_2, (b) TiO_2 wt.% against FeO_{total}/MgO, (c) TiO_2 wt.% against V (ppm), and (d) Yb (ppm) against V (ppm). The Cuban Moa-Baracoa Ophiolite-related basaltic rocks (MBOB) include the backarc basalts G1 group (Marchesi *et al*. 2007). The Hispaniola ophiolite-related mafic rocks from Gaspar Hernandez complex (Escuder-Viruete *et al*. 2011a). The fields of forearc basalts, transitional lavas, and boninite lavas from Izu-Bonin-Mariana volcanic arc (Reagan *et al*. 2010; Stern *et al*. 2012) are also plotted for comparison. Basalts from the East Pacific Rise are illustrated in the grey-line field. Data and references for these sample suites are from the PetDB data base (http://www.petdb.org/).

7.3. Model for generation of the La Tinta ultramafic mélange and implications for the Caribbean tectonic evolution

In the La Tinta mélange FAB-related amphibolites were recognized. Many of the amphibolites (ca. 123 Ma $^{40}Ar/^{39}Ar$ cooling age) are of doleritic nature and recrystallized at low pressure (3.8 kbar, 720ºC for the Cpx-bearing samples). These amphibolites are comparable with mafic rocks of the Gaspar Hernandez serpentinized peridotite, which were considered by Escuder-Viruete *et al*. (2011a) as MOR basalts formed in the proto-Caribbean oceanic lithosphere. We hence suggest that the Gaspar Hernandez mafic rocks, which are metamorphosed to seemingly comparable low-pressure conditions in the greenschist and lower amphibolite facies (Escuder-Viruete *et al*. 2011a), formed, instead, in the Caribbean forearc. These considerations allow us to suggest that the amphibolitic blocks from the La Tinta mélange correspond to fragments of the proto-forearc spreading lithosphere (Figure 16).

Subduction initiation started in the Pacific realm in the Early Cretaceous (~132 Ma, Rojas-Agramonte *et al*. 2011), perhaps along a pre-existing weak zone, a collapsed transform, in the oceanic crust (Pindell *et al*. 2012; Whattam and Stern 2015) (Figure 16(a)). The FAB crust formed by upwelling of fertile asthenosphere at the beginning of subsidence or sinking of the Proto-Caribbean plate, with no interaction with slab-derived fluids/melts (Stern 2004; Stern *et al*. 2012) (Figure 16 (b)). Whattam and Stern (2011) described the upwelling fertile asthenosphere in the forearc setting, nil slab-derived fluids with which to interact. They described a seafloor spreading along the margin of the upper plate simultaneously with the MORB/FAB tholeiites formation as the oceanic lithosphere would start to sink. Following these authors, this seafloor spreading occurs as asthenosphere floods over the sinking plate into the widening void above, which

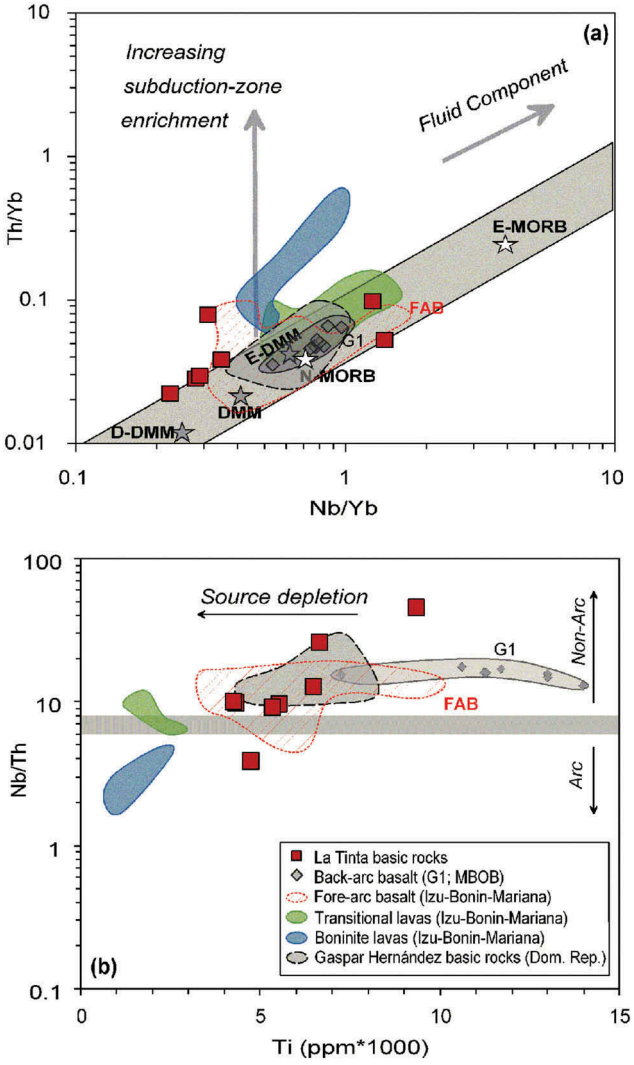

Figure 14. (a) Th/Yb *versus* Nb/Yb and (b) Nb/Th *versus* Ti (ppm*1000) plots for the La Tinta amphibolite blocks. Fields for comparison as in Figure 14. NMORB and EMORB after Sun and McDonough (1989), and depleted MORB mantle (DMM), depleted-DMM (D-DMM), and enriched-DMM (E-DMM) after Workman and Hart (2005).

melts due to decompression. This stage would be represented by the dolerite-derived amphibolite protoliths from the La Tinta mélange. They were later metamorphosed at high temperature and low pressure in a static ocean floor metamorphic environment and cooled, below the retention temperature of Ar in metamorphic amphibole, at ca. 123 Ma shortly after their intrusion in the forearc mantle. The formation of the FAB and related rocks then produced a very depleted mantle residue. This very depleted mantle residue interacts later with slab-derived fluids yielding boninites and boninitic affinity rocks, probably represented in the nearby Hispaniola, by the harzburgites and the boninitic gabbros reported in the Puerto Plata complex and the boninitic sequences of the Maimón formation

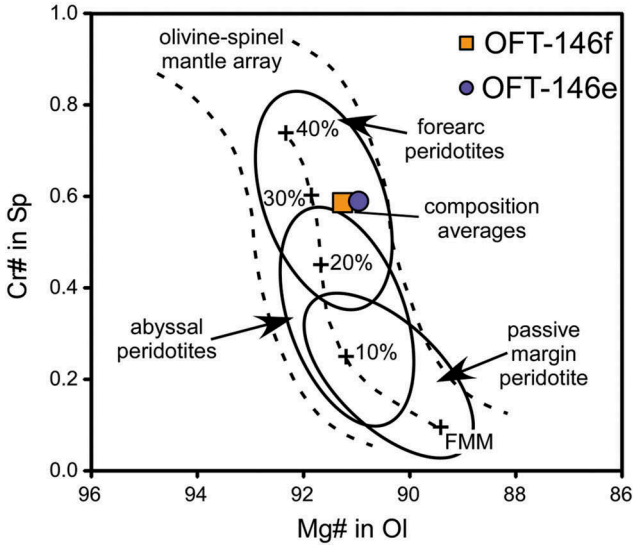

Figure 15. Mg# in olivine *versus* Cr# in spinel showing the average composition of minerals from ultramafic rocks.

(Escuder-Viruete *et al.* 2006, 2014) (Figure 16(c)). The hydration in forearc position, due to normal faulting, produces the low-the pressure metamorphism of mafic sills/dikes and serpentinization of ultramafic rocks (Figure 16(d)). The final collision of the Greater Antilles arc (leading edge of the Caribbean plate) against the North American continent, the obduction and emplacement of ophiolitic complexes as well as synorogenic basin development (70–65 Ma; Iturralde-Vinent *et al.* 2006) produces the breaking of metamorphosed dolerite dikes and sills embedded in the serpentinitic mélange (Figure 16(e)).

8. Conclusions

The amphibolite (Amp+Pl±Cpx) blocks from La Tinta mélange have MORB-like trace element compositions with a slight subduction zone imprint, similar to most FABs worldwide. Spinel and olivine mineral chemistry of the enclosing serpentinized ultramafic rocks suggests a forearc position for these rocks. Textures and whole rock and mineral compositions of amphibolites and metaultramafics, along with $^{40}Ar/^{39}Ar$ amphibole data indicate a metamorphic cooling age of 123.2 ± 2.2 Ma, thus suggesting that the amphibolites represent sheeted dikes/sills intruded in the forearc region during the earliest stages (Early Cretaceous) of subduction in the Caribbean realm. The FAB-related compositions of the protoliths of the amphibolite blocks correlate with the Gaspar Hérnandez complex of Hispaniola, indicating a belt of forearc complexes of Early Cretaceous age in eastern Cuba and northern Hispaniola. The La Tinta FAB-related amphibolite blocks correspond to fragments of

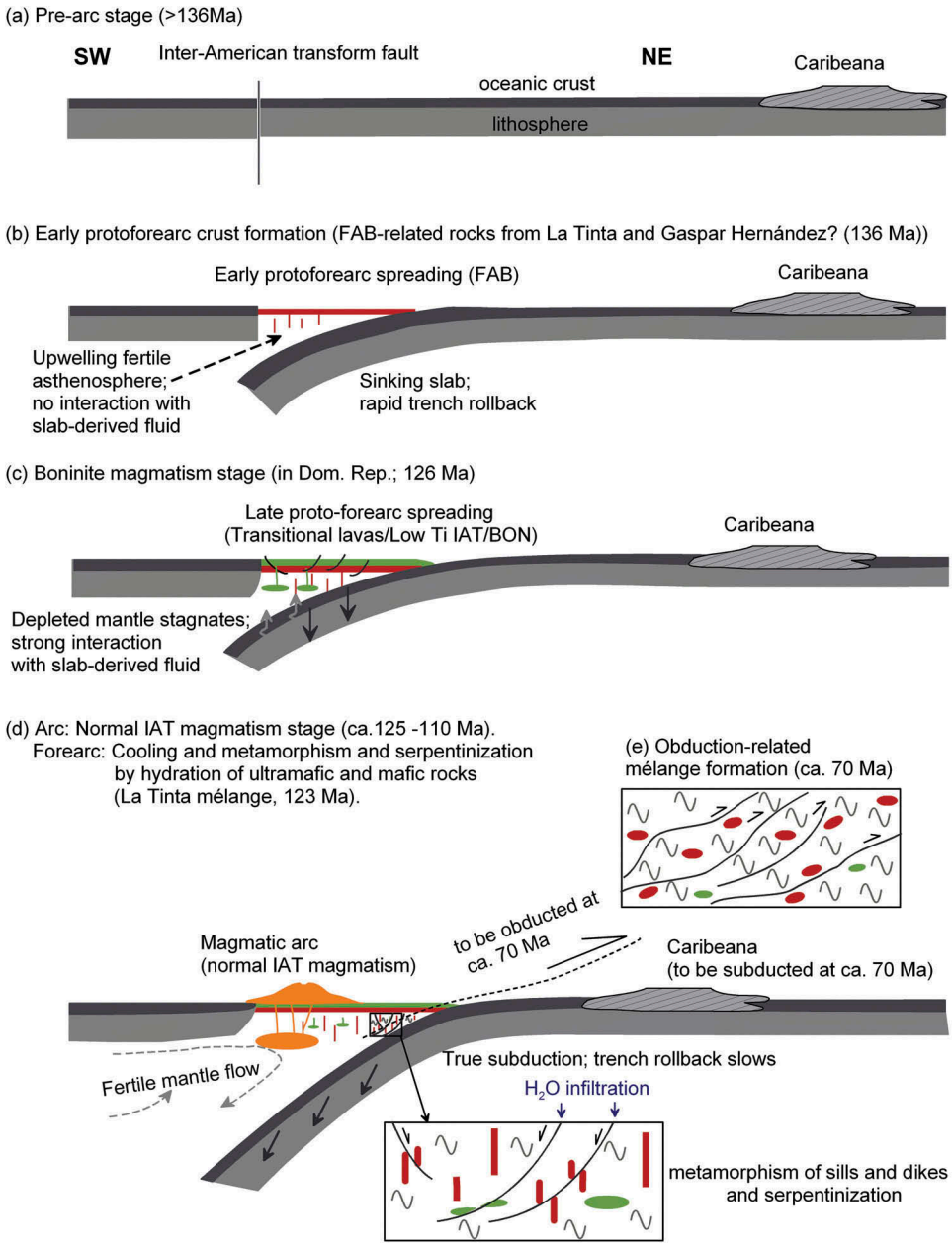

Figure 16. Simplified model for the generation of the Early Cretaceous Caribbean island-arc based on the model of Stern *et al*. (2012) and adapted from Escuder-Viruete *et al*. (2014), and tectonomagmatic evolution of the La Tinta serpentinitic mélange. (a) Subduction initiated in the Pacific realm, perhaps along a pre-existing weak zone, a collapsed transform, in the oceanic lithosphere (Pindell *et al*. 2012; Whattam and Stern 2015). (b) Initiation of slab subsidence and upwelling of fertile asthenospheric mantle produce forearc basalts and related sills and dikes (represented by amphibolites from La Tinta mélange, Cuba). (c) The interaction with slab-derived fluids/melts allows the residual depleted mantle to produce boninitic melts and related boninitic rocks. (d) Slab rollback slows and causes flow of a fertile mantle, which interacts with slab-derived fluids/melts to produce normal IAT. The hydration in forearc position produces the low-pressure metamorphism of basic sills and dikes, and serpentinization of ultramafic rocks. (e) The final NE-directed ophiolitic complexes obduction, emplacement, collision, and synorogenic basin development produces breaking of metamorphosed sills and dikes embedded in the serpentinites (70–65 Ma), yielding the mélange formation.

the proto-forearc spreading lithosphere in a subduction initiation scenario in the Pacific realm (ca. 136 Ma) formed by upwelling of the fertile asthenosphere. This event occurred at the onset of subduction of the Proto-Caribbean with no interaction with a slab-derived component, yielding a depleted mantle residue. Later, this depleted mantle residue interacted with slab-derived fluids to produce boninitic magmas. The dikes and sills cooled and metamorphosed at low pressure (~3.8 kbar, 12 km depth, <720ºC) at ca. 123 Ma. At this stage, the mélange started to form during normal faulting of the forearc and serpentinization of the mantle. In a late

stage of the tectonic evolution of the region (ca. 70 Ma), the forearc obducted onto the evolving collision wedge triggered by the subduction of the Caribeana terrane, resulting in a further development of the serpentinitic mélange.

Acknowledgements

The authors thank Jose Maria Gonzalez Jimenez and two anonymous reviewers for their in-depth reviews and suggestions, and the editor Robert J. Stern for the useful comments and suggestions, which substantially improved the paper. In addition, Manuel A. Iturralde-Vinent is acknowledged. We thank the ARGONAUT laboratory team (Salzburg, Austria) for technical assistance during Ar-dating and A. Rodríguez-Vega for field assistance.

Disclosure statement

No potential conflict of interest was reported by the authors.

Funding

We appreciate financial support from Spanish MINECO projects [CGL2009-12446 and CGL2012-36263] (co-financed by Fondo Europeo de Desarrollo Regional: FEDER). The University of Granada is thanked for co-funding the chemical analyses. IBQ appreciates the FAPA project from Vicerrectorado de Investigación (Uniandes) for financial support.

References

Arai, S., 1992, Chemistry of chromian spinel in volcanic rocks as a potential guide to magma chemistry: Mineralogical Magazine, v. 56, p. 173–184. doi:10.1180/minmag

Blanco-Quintero, I.F., Garcia-Casco, A., Rojas-Agramonte, Y., Rodriguez-Vega, A., Lázaro, C., and Iturralde-Vinent, M.A., 2010, Metamorphic evolution of subducted hot oceanic crust (La Corea Mélange, Cuba): American Journal of Science, v. 310, p. 889–915. doi:10.2475/11.2010.01

Blanco-Quintero, I.F., Proenza, J.A., Garcia-Casco, A., Tauler, E., and Galí, S., 2011a, Serpentinites and serpentinites within a fossil subduction channel: La Corea mélange, eastern Cuba: Geologica Acta, v. 9, no. 3–4, p. 389–405.

Blanco-Quintero, I.F., Rojas-Agramonte, Y., Garcia-Casco, A., Kröner, A., Mertz, D.F., Lázaro, C., Blanco-Moreno, J., and Renne, P.R., 2011b, Timing of subduction and exhumation in a subduction channel: Evidence from slab melts from La Corea mélange (eastern Cuba): Lithos, v. 127, p. 86–100. doi:10.1016/j.lithos.2011.08.009

Boiteau, A., Michard, A., and Saliot, P., 1972, Métamorphisme de haute pression dans le complexe ophiolitique du Purial (Oriente, Cuba): Comptes Rendus de l'Académie des Sciences Paris, v. 274, (série D), p. 2137–2140.

Cárdenas-Párraga, J., Garcia-Casco, A., Harlow, G.E., Blanco-Quintero, I.F., Rojas-Agramonte, Y., and Kröner, A., 2012, Hydrothermal origin and age of jadeitites from Sierra del Convento Mélange (Eastern Cuba): European Journal of Mineralogy, v. 24, p. 313–331. doi:10.1127/0935-1221/2012/0024-2171

Cobiella, J., 1974, Los Macizos Serpentiníticos de Sabanilla, Mayarí Arriba: Oriente: Revista Tecnológica, v. 12, no. 4, p. 41–50.

Cobiella, J., Campos, M., Boiteau, A., and Quintas, F., 1977, Geología del Flanco Sur de la Sierra del Purial: Revista La Minería en Cuba, v. 3, no. 1, p. 54–62.

Cobiella, J., Quintas, F., Campos, M., and Hernández, M., 1984, Geología de la región central y suroriental de la provincia de Guantánamo. Santiago de Cuba: Editorial Oriente, 125 p.

Cobiella-Reguera, J.L., 2005, Emplacement of Cuban ophiolites: Geological Acta, v. 3, p. 273–294.

Connolly, J.A.D., 2005, Computation of phase equilibria by linear programming: A tool for geodynamic modeling and its application to subduction zone decarbonation: Earth and Planetary Science Letters, v. 236, p. 524–541. doi:10.1016/j.epsl.2005.04.033

Dale, J., Powell, R., White, R.W., Elmer, F.L., and Holland, T.J.B., 2005, A thermodynamic model for Ca-Na clinoamphiboles in Na2O-CaO-FeO-MgO-Al2O3-SiO2-H2O-O for petrological calculations: Journal of Metamorphic Geology, v. 23, p. 771–791. doi:10.1111/jmg.2005.23.issue-8

D'Antonio, M., and Kristensen, M.B., 2004, Serpentine and brucite of ultramafic clasts from the South Chamorro Seamount (Ocean Drilling Program Leg 195, Site 1200): Inferences for the serpentinization of the Mariana forearc mantle: Mineralogical Magazine, v. 68, no. 6, p. 887–904. doi:10.1180/0026461046860229

Escuder-Viruete, J., Castillo-Carrión, M., and Pérez-Estaún, A., 2014, Magmatic relationships between depleted mantle harzburgites, boninitic cumulate gabbros and subduction-related tholeiitic basalts in the Puerto Plata ophiolitic complex, Dominican Republic: Implications for the birth of the Caribbean island-arc: Lithos, v. 196-197, p. 261–280. doi:10.1016/j.lithos.2014.03.013

Escuder-Viruete, J., Contreras, F., Joubert, M., Urien, P., Stein, G., Weis, D., and Pérez-Estaún, A., 2007, Tectónica y geoquímica de la Formación Amina: Registro del arco isla Caribeño primitivo en la Cordillera Central, República Dominicana: Boletín Geológico y Minero, 118, no. 2, p. 221–242.

Escuder-Viruete, J., Díaz De Neira, A., Hernáiz Huerta, P.P., Monthel, J., Garcia Senz, J., Joubert, M., Lopera, E., Ullrich, T., Friedman, R., Mortensen, J., and Pérez-Estaún, A., 2006, Magmatic relationships and ages of Caribbean island arc tholeiites, boninites and related felsic rocks, Dominican Republic: Lithos, v. 90, p. 161–186. doi:10.1016/j.lithos.2006.02.001

Escuder-Viruete, J., Friedman, R., Castillo-Carrión, M., Gabites, J., and Pérez-Estaún, A., 2011a, Origin and significance of the ophiolitic high-P mélanges in the northern Caribbean convergent margin: Insights from the geochemistry and large-scale structure of the Río San Juan metamorphic complex: Lithos, v. 127, p. 483–504. doi:10.1016/j.lithos.2011.09.015

Escuder-Viruete, J., Pérez-Estaún, A., Gabites, J., and Suárez-Rodríguez, Á., 2011b, Structural development of a high-pressure collisional accretionary wedge: The Samaná complex, northern Hispaniola: Journal of Structural Geology, v. 33, p. 928–950. doi:10.1016/j.jsg.2011.02.006

Escuder-Viruete, J., Pérez-Estaún, A., Weis, D., and Friedman, R., 2010, Geochemical characteristics of the Río Verde complex,

central Hispaniola: Implications for the paleotectonic reconstruction of the Lower Cretaceous Caribbean island-arc: Lithos, v. 114, p. 168–185. doi:10.1016/j.lithos.2009.08.007

Escuder-Viruete, J., Valverde-Vaquero, P., Rojas-Agramonte, Y., Gabites, J., and Carrion Castillo, M., 2013a, Timing of deformational events in the Río San Juan complex: Implications for the tectonic controls on the exhumation of high-P rocks in the northern Caribbean subduction–accretionary prism: Lithos, v. 177, p. 416–435. doi:10.1016/j.lithos.2013.07.006

Escuder-Viruete, J., Valverde-Vaquero, P., Rojas-Agramonte, Y., Gabites, J., and Pérez-Estaún, A., 2013b, From intra-oceanic subduction to arc accretion and arc–continent collision: Insights from the structural evolution of the Río San Juan metamorphic complex, northern Hispaniola: Journal of Structural Geology, v. 46, p. 34–56. doi:10.1016/j.jsg.2012.10.008

Fonseca, E., González, R., Delgado, R., and Savieleva, G., 1989, Presencia de efusivos y ofiolíticos y de boninitas en las provincias de La Habana y Matanzas: Boletín Técnico, Geología, v. 1, p. 1–9.

Garcia-Casco, A., Iturralde-Vinent, M.A., and Pindell, J., 2008a, Latest Cretaceous collision/ accretion between the Caribbean Plate and Caribeana: Origin of metamorphic terranes in the Greater Antilles: International Geology Review, v. 50, p. 781–809. doi:10.2747/0020-6814.50.9.781

Garcia-Casco, A., Lázaro, C., Rojas-Agramonte, Y., Kröner, A., Torres-Roldan, R.L., Núñez, K., Neubauer, F., Millan, G., and Blanco-Quintero, I., 2008b, Partial melting and counterclockwise P T path of subducted oceanic crust (Sierra del Convento Mélange, Cuba): Journal of Petrology, v. 49, p. 129–161. doi:10.1093/petrology/egm074

Garcia-Casco, A., Rodríguez Vega, A., Cárdenas Párraga, J., Iturralde-Vinent, M.A., Lázaro, C., Blanco Quintero, I., Rojas-Agramonte, Y., Kröner, A., Núñez Cambra, K., Millán, G., Torres-Roldán, R.L., and Carrasquilla, S., 2009, A new jadeitite jade locality (Sierra del Convento, Cuba): First report and some petrological and archeological implications: Contributions to Mineralogy and Petrology, v. 158, p. 1–16. doi:10.1007/s00410-008-0367-0

Garcia-Casco, A., Torres-Roldán, R.L., Iturralde-Vinent, M.A., Millán, G., Núñez Cambra, K., Lázaro, C., and Rodríguez Vega, A., 2006, High pressure metamorphism of ophiolites in Cuba: Geologica Acta, v. 4, p. 63–88.

Gervilla, F., Proenza, J.A., Frei, R., González-Jiménez, J.M., Garrido, C.J., Melgarejo,, J.C., Meibom, A., Díaz-Martínez, R., and Lavaut, W., 2005, Distribution of platinum-group elements and Os isotopes in chromite ores from Mayarí-Baracoa Ophiolitic Belt (eastern Cuba): Contributions to Mineralogy and Petrology, v. 150, p. 589–607. doi:10.1007/s00410-005-0039-2

Govindaraju, K., 1994, Compilation of working values and sample description for 383 geostandards: Geostandards Newsletter, v. 18, p. 1–158. doi:10.1111/j.1751-908X.1994.tb00502.x

Gradstein, F.M., and Ogg, J.G., 2005, Time scale encyclopedia of geology: v. 5, Oxford, United Kingdom Elsevier Academic Press.

Green, E., Holland, T., and Powell, R., 2007, An order-disorder model for omphacitic pyroxenes in the system jadeite-diopside-hedenbergite-acmite, with applications to eclogitic rocks: American Mineralogist, v. 92, p. 1181–1189. doi:10.2138/am.2007.2401

Gyarmati, P., and Leyé O'Conor, J., 1990, Informe final sobre los trabajos de levantamiento geológico en escala 1:50000 y busqueda acompañante en el poligono CAME V, Guantánamo: Cuba, Oficina Nacional de Recursos Minerales.

Gyarmati, P., Méndez, I., and Lay, M., 1997, Caracterización de las rocas del arco de islas Cretácico en la Zona Estructuro-Facial Nipe-Cristal-Baracoa, *in* Furrazola, G.F., and Nuñez-Cambra, K.E., eds., Estudios sobre Geología de Cuba: Ciudad de la Habana, Cuba, Instituto de Geología y Paleontología, p. 357–364.

Handler, R., Neubauer, F., Velichkova, S.H., and Ivanov, Z., 2004, $^{40}Ar/^{39}Ar$ age constraints on the timing of magmatism and post-magmatic cooling in the Panagyurishte region, Bulgaria: Schweizerische Mineralogische und Petrographische Mitteilungen, v. 84, p. 119–132.

Harrison, T.M., 1981, Diffusion of ^{40}Ar in hornblende: Contributions to Mineralogy and Petrology, v. 78, p. 324–331. doi:10.1007/BF00398927

Hart, S.R., and Zindler, A., 1986, In search of a bulk-Earth composition: Chemical Geology, v. 57, no. 3–4, p. 247–267. doi:10.1016/0009-2541(86)90053-7

Hattori, K.H., and Guillot, S., 2007, Geochemical character of serpentinites associated with high- to ultrahigh-pressure metamorphic rocks in the Alps, Cuba, and the Himalayas: Recycling of elements in subduction zones: Geochemistry, Geophysics, Geosystems, v. 8, p. Q09010. doi:10.1029/2007GC001594

Hey, M.H., 1954, A new review of the chlorites: Mineralogical Magazine, v. 30, p. 277–292. doi:10.1180/minmag.1954.030.224.01

Hickey, R., and Frey, F.A., 1982, Geochemical characteristics of boninite series volcanics: Implications for their source: Geochimica et Cosmochimica Acta, v. 46, p. 2099–2115. doi:10.1016/0016-7037(82)90188-0

Holland, T., Baker, J., and Powell, R., 1998, Mixing properties and activity-composition relationships of chlorites in the system MgO-FeO-Al2O3-SiO2-H2O: European Journal of Mineralogy, v. 10, p. 395–406. doi:10.1127/ejm/10/3/0395

Holland, T., and Powell, R., 1996, Thermodynamics of order-disorder in minerals. 2. Symmetric formalism applied to solid solutions: American Mineralogist, v. 81, p. 1425–1437.

Holland, T., and Powell, R., 1998, An internally consistent thermodynamic data set for phases of petrological interest: Journal of Metamorphic Geology, v. 16, p. 309–343. doi:10.1111/j.1525-1314.1998.00140.x

Horan, S.L., 1995, The geochemistry and tectonic significance of the Maimon-Amina schists, Cordillera, Dominican Republic [M.S. thesis]: Gainesville, University of Florida, 172 p.

Ishizuka, O., Tani, K., and Reagan, M.K., 2014, Izu-Bonin-Mariana forearc crust as a modern ophiolite analogue: Elements, v. 10, p. 115–120. doi:10.2113/gselements.10.2.115

Ishizuka, O., Tani, K., Reagan, M.K., Kanayama, K., Umino, S., Harigane, Y., Sakamoto, I., Miyajima, Y., Yuasa, M., and Dunkley, D.J., 2011, The time scales of subduction initiation and subsequent evolution of an oceanic island arc: Earth and Planetary Science Letters, v. 306, p. 229–240. doi:10.1016/j.epsl.2011.04.006

Iturralde-Vinent, M., 1976, Estratigrafía de la Zona Calabazas-Achotal, Mayarí Arriba, Oriente: Revista La Minería En Cuba, v. 1, no. 5, p. 9–23.

Iturralde-Vinent, M.A., 1996a, Introduction to cuban geology and geophysics, *in* Iturralde-Vinent, M.A., ed., Ofiolitas y Arcos Volcánicos de Cuba: Miami, USA, IGCP Project 364 Special Contribution 1, p. 3–35.

Iturralde-Vinent, M.A., 1996b, Geología de las ofiolitas de Cuba, *in* Iturralde-Vinent, M.A., ed., Ofiolitas y Arcos Volcánicos de Cuba: Miami, USA, IGCP Project 364 Special Contribution 1, p. 83–120.

Iturralde-Vinent, M.A., 1998, Sinopsis de la Constitución Geológica de Cuba: Acta Geológica Hispánica, v. 33, p. 9–56.

Iturralde-Vinent, M.A., Díaz Otero, C., Garcia-Casco, A., and Van Hinsbergen, D., 2008, Paleogene Foredeep Basin deposits of North-Central Cuba: A record of Arc-Continent collision between the Caribbean and North American Plates: International Geology Review, v. 50, p. 863–884. doi:10.2747/0020-6814.50.10.863

Iturralde-Vinent, M.A., Díaz-Otero, C., Rodríguez-Vega, A., and Díaz-Martínez, R., 2006, Tectonic implications of paleontologic dating of Cretaceous-Danian sections of Eastern Cuba: Geologica Acta, v. 4, p. 89–102.

Jolly, W.T., and Lidiak, E.G., 2006, Role of crustal meeting in petrogenesis of the Cretaceous water Island formation (Virgin Islands, northeast Antilles Island Arc): Geologica Acta, v. 4, p. 7–34.

Kerr, A.C., Iturralde-Vinent, M., Saunders, A.D., Babbs, T.L., and Tarney, J., 1999, A new plate tectonic model of the Caribbean: Implications from a geochemical reconnaissance of Cuban Mesozoic volcanic rocks: Geological Society of America Bulletin, v. 111, p. 1581–1599. doi:10.1130/0016-7606(1999)111<1581:ANPTMO>2.3.CO;2

Kesler, S.E., Campbell, I.H., and Allen, C.M., 2005, Age of the Los Ranchos Formation, Dominican Republic: Timing and tectonic setting of primitive island arc volcanism in the Caribbean region: Geological Society of America Bulletin, v. 117, p. 987–995. doi:10.1130/B25594.1

Knipper, A.L., and Cabrera, R., 1974, Téctonica y geología histórica de la zona de articulación entre el mio- y eugeosinclinal y del cinturón hiperbasítico de Cuba: Habana, Instituto de GeologíDa y Paleontologia. Contribución a la Geología de Cuba, p. 15–77.

Krebs, M., Maresch, W.V., Schertl, H.-P., Baumann, A., Draper, G., Idlemann, B., Münker, C., and Trapp, E., 2008, The dynamics of intra-oceanic subduction zones: A direct comparison between fossil petrological evidence (Rio San Juan Complex, Dominican Republic) and numerical simulation: Lithos, v. 103, p. 106–137. doi:10.1016/j.lithos.2007.09.003

Krebs, M., Schertl, H.-P., Maresch, W.V., and Draper, G., 2011, Mass flow in serpentinite-hosted subduction channels: P–T–t path patterns of metamorphic blocks in the Rio San Juan mélange (Dominican Republic): Journal of Asian Earth Sciences, v. 42, no. 4, p. 569–595. doi:10.1016/j.jseaes.2011.01.011

Lázaro, C., Blanco-Quintero, I.F., Rojas-Agramonte, Y., Proenza, J.A., Núñez-Cambra, K., and Garcia-Casco, A., 2013, First description of a metamorphic sole related to ophiolite obduction in the northern Caribbean: Geochemistry and petrology of the Güira de Jauco Amphibolite Complex (eastern Cuba) and tectonic implications: Lithos, v. 179, p. 193–210. doi:10.1016/j.lithos.2013.08.019

Lázaro, C., and Garcia-Casco, A., 2008, Geochemical and Sr-Nd isotope signatures of pristine slab melts and their residues (Sierra del Convento mélange, eastern Cuba): Chemical Geology, v. 255, p. 120–133. doi:10.1016/j.chemgeo.2008.06.017

Lázaro, C., Garcia-Casco, A., Blanco-Quintero, I.F., Rojas-Agramonte, Y., Corsini, M., and Proenza, J.A., 2015, Did the Turonian–Coniacian plume pulse trigger subduction initiation in the Northern Caribbean? Constraints from 40Ar/39Ar dating of the Moa-Baracoa metamorphic sole (eastern Cuba): International Geology Review, v. 57, no. 5–8, p. 919–942. doi:10.1080/00206814.2014.924037

Lázaro, C., Garcia-Casco, A., Rojas Agramonte, Y., Kröner, A., Neubauer, F., and Iturralde-Vinent, M., 2009, Fifty-five million-year history of oceanic subduction and exhumation at the northern edge of the Caribbean plate (Sierra del Convento mélange, Cuba): Journal of Metamorphic Geology, v. 27, p. 19–40. doi:10.1111/j.1525-1314.2008.00800.x

Leake, B.E., Woolley, A.R., Arps, C.E.S., Birch, W.D., Gilbert, M.C., Grice, J.D., Hawthorne, F.C., Kato, A., Kisch, H.J., Krivovichev, V.G., Linthout, K., Laird, J., Mandarino, J.A., Maresch, W.V., Nickel, E.H., Rock, N.M.S., Schumacher, J.C., Smith, D.C., Stephenson, N.C.N., Ungaretti, L., Whittaker, E.J.W., and Touzhi, G., 1997, Nomenclature of amphiboles: Report of the subcommittee on Amphiboles of the international mineralogical association, commission on new minerals and mineral names: American Mineralogist, v. 82, p. 1019–1037.

Lewis, G.E., and Straczek, J.A., 1955, Geology of South-Central Oriente Province, Cuba: US Geological Survey Bulletin, v. 975-D, p. 171–336.

Lewis, J.F., Astacio, V.A., Espaillat, J., and Jiménez, J., 2000, The occurrence of volcanogenic massive sulfide deposits in the Maimón Formation, Dominican Republic: The Cerro de Maimón, Loma Pesada and Loma Barbuito deposits, *in* Sherlock, R., Barsch, R., and Logan, A., eds., VMS deposits of Latin America: Geological Society of Canada Special Publicationv. 2, p. 213–239.

Lewis, J.F., Escuder Viruete, J., Hernaiz Huerta, P.P., Gutierrez, G., Draper, G., and Pérez-Estaún, A., 2002, Geochemical subdivision of the Circum-Caribbean Island arc, Dominican Cordillera Central: Implications for crustal formation, accretion and growth within an intra-oceanic setting: Acta Geológica Hispánica, 37, no. 2–3, p. 81–122.

Ludwig, K.R., 2001, Isoplot/Ex – A geochronological toolkit for microsoft excel: Special Publication No 1a, Berkley, Berkeley Geochronological Center.

Marchesi, C., Garrido, C.J., Bosch, D., Proenza, J.A., Gervilla, F., Monie, P., and Rodriguez-Vega, A., 2007, Geochemistry of Cretaceous magmatism in eastern Cuba: Recycling of North American continental sediments and implications for subduction polarity in the Greater Antilles Paleo-arc: Journal of Petrology, v. 48, p. 1813–1840. doi:10.1093/petrology/egm040

Marchesi, C., Garrido, C.J., Godard, M., Proenza, J.A., Gervilla, F., and Blanco-Moreno, J., 2006, Petrogenesis of highly depleted peridotites and gabbroic rocks from the Mayarí-Baracoa Ophiolitic Belt (eastern Cuba): Contributions to Mineralogy and Petrology, v. 151, p. 717–736. doi:10.1007/s00410-006-0089-0

McDonough, W.F., and Sun, -S.-S., 1995, The composition of the Earth: Chemical Geology, v. 120, p. 223–253. doi:10.1016/0009-2541(94)00140-4

McDougall, I., and Harrison, T.M., 1999, Geochronology and Thermochronology by the 40Ar / 39Ar Method: Oxford, Oxford University Press.

Millán, G., Somin, M.L., and Díaz, C., 1985, Nuevos datos sobre la geología del macizo montañoso de la Sierra del Purial, Cuba Oriental: Reporte de Investigación del Instituto de Geología y Paleontología, v. 2, p. 52–74.

Monthel, J., 2010, Mapa Geológico de la Hoja a E. 1:50.000 nº 6075-I (Puerto Plata). Proyecto SYSMIN de Cartografía Geotemática de la República Dominicana. Programa: Santo Domingo, Dirección General de Minería, 310 p.

Morimoto, N., Fabries, J., Ferguson, A.K., Ginzburg, I.V., Ross, M., Seifert, F.A., Zussman, J., Aoki, K., and Gottardi, G., 1988, Nomenclature of pyroxenes: Report of the Subcommittee on Pyroxenes of the international mineralogical association, commission on new minerals and mineral names: American Mineralogist, v. 73, p. 1123–1133.

Newton, R.C., Charlu, T.V., and Kleppa, O.J., 1980, Thermochemistry of the high structural state plagioclases: Geochemica Cosmochimica Acta, v. 44, p. 933–941. doi:10.1016/0016-7037(80)90283-5

Núñez-Cambra, K.E., Garcia-Casco, A., Iturralde-Vinent, M.A., and Millán, G., 2004, Emplacement of the ophiolite complex in Eastern Cuba, *in* 32nd International Geological Congress, Session G20.11 Caribbean Plate Tectonics: Florencia, Proceedings, CD-rom.

Pearce, J.A., 1976, Statistical analysis of major element patterns in basalts: Journal of Petrology, v. 17, p. 15–43. doi:10.1093/petrology/17.1.15

Pearce, J.A., 2003, Supra-subduction zone ophiolites: The search for modern analogues, *in* Dilek, Y., and Newcomb, S., eds., Ophiolite concept and the evolution of geological thought: Geological Society of America Special Paper, v. 373, p. 269–293.

Pearce, J.A., 2014, Immobile element Fingerprinting of Ophiolites: Elements, v. 10, no. 2, p. 101–108. doi:10.2113/gselements.10.2.101

Pearce, J.A., and Stern, R.J., 2006, The Origin of Back-arc Basin Magmas: Trace element and isotopic perspectives, *in* Christie, D.M., Fisher, C.R., Lee, S.-M., and Givens, S., eds., Back-Arc spreading systems: Geological, biological, chemical, and physical interactions: AGU monograph 166, Washington DC, American Geophysical Union, p. 63–86.

Pindell, J.L., Cande, S.C., Pitman, W.C., Rowley, D.B., Dewey, J.F., Labrecque, J., and Haxby, W., 1988, A plate-kinematic framework for models of Caribbean evolution: Tectonophysics, v. 155, p. 121–138. doi:10.1016/0040-1951(88)90262-4

Pindell, J.L., Maresch, W.V., Martens, U., and Stanek, K.P., 2012, The greater antillean arc: Early Cretaceous origin and proposed relationship to Central American subduction mélanges: Implications for models of Caribbean evolution:: International Geology Review, v. 54, p. 131–143. doi:10.1080/00206814.2010.510008

Proenza, J., Gervilla, F., Melgarejo, J.C., and Bodinier, J.-L., 1999, Al- and Cr-rich chromitites from the Mayari-Baracoa ophiolitic belt (eastern Cuba); consequence of interaction between volatile-rich melts and peridotites in suprasubduction mantle: Economic Geology, v. 94, p. 547–566. doi:10.2113/gsecongeo.94.4.547

Proenza, J.A., Díaz-Martínez, R., Iriondo, A., Marchesi, C., Melgarejo, J.C., Gervilla, F., Garrido, C.J., Rodríguez-Vega, A., Lozano-Santacruz, R., and Blanco-Moreno, J.A., 2006, Primitive island-arc Cretaceous volcanic rocks in eastern Cuba: The Téneme Formation: Geologica Acta, v. 4, p. 103–121.

Pushcharovsky, Y., ed., 1988, Mapa geológico de la República de Cuba escala 1:250 000: Havana, Cuba/Moscow, USSR. Academy of Sciences of Cuba and Academy of Sciences of USSR.

Quintas, F., 1987, Formación Mícara en Yumurí Arriba, Baracoa, clave para la interpretación de la Geología Histórica Pre-Paleocénica de Cuba Oriental: Revista Geología y Minería, 5, no. 3, p. 3–20.

Quintas, F., 1988, Características estratigráficas y estructurales del complejo ofiolítico y eugeosinclinal de la cuenca del Río Quibiján, Baracoa: Minería y Geología, v. 6, p. 11–22.

Quintas, F., 1989, Análisis estratigráfico y paleogeografía del Cretácico superior y del Paleógeno de la provincia de Guantánamo y áreas cercanas [Doctoral thesis]: Holguín, Cuba, Instituto Superior Minero Metalúrgico de Moa., 161 p.

Reagan, M.K., Ishizuka, O., Stern, R.J., Kelley, K.A., Ohara, Y., Blichert-Toft, J., Bloomer, S.H., Cash, J., Fryer, P., Hanan, B.B., Hickey-Vargas, R., Ishii, T., Kimura, J.I., Peate, D.W., Rowe, M. C., and Woods, M., 2010, Fore-arc basalts and subduction initiation in the Izu-Bonin-Mariana system: Geochemistry, Geophysics, Geosystems, v. 11, p. Q03X12. doi:10.1029/2009GC002871

Rojas-Agramonte, Y., Kröner, A., Garcia-Casco, A., Iturralde-Vinent, M.A., Somin, M., Mattinson, J.M., Millán Trujillo, G., Sukar, K., Pérez Rodríguez, M., and Wingate, M.T.D., 2011, Timing and evolution of Cretaceous Island Arc magmatism in Central Cuba: Implications for the history of arc systems in the Northwestern Caribbean: Journal of Geology, v. 119, p. 619–640. doi:10.1086/662033

Rollinson, H.R., 1983, The geochemistry of Mafic and Ultramafic rocks from the Archaean Greenstone Belts of Sierra Leone: Mineralogical Magazine, v. 47, p. 267–280. doi:10.1180/minmag

Somin, M.L., Arakelyants, M.M., and Kolesnikov, E.M., 1992, Age and tectonic significance of high-pressure metamorphic rocks in Cuba: International Geology Review, v. 34, p. 105–118. doi:10.1080/00206819209465587

Somin, M.L., and Millán, G., 1981, Geology of the metamorphic complexes of Cuba (in russian): Moscow, Nauka, 219 p.

Steiger, R.H., and Jäger, E., 1977, Subcommission on geochronology: Convention on the use of decay constants in geo- and cosmochronology: Earth and Planetary Science Letters, v. 36, p. 359–362. doi:10.1016/0012-821X(77)90060-7

Stern, R.J., 2004, Subduction initiation: Spontaneous and induced: Earth and Planetary Science Letters, v. 226, p. 275–292. doi:10.1016/S0012-821X(04)00498-4

Stern, R.J., Reagan, M., Ishizuka, O., Ohara, Y., and Whattam, S., 2012, To understand subduction initiation, study forearc crust: To understand forearc crust, study ophiolites: Lithosphere, v. 4, p. 469–483. doi:10.1130/L183.1

Sun, S.S., and McDonough, W.F., 1989, Chemical and isotope systematics of oceanic basalts: Implications for mantle composition and processes, *in* Saunders, A.D., and Norry, M.J., Eds., Magmatism in Ocean Basins: Geological Society of London Special Publication, Vol. 42, p. 313–345.

Torrez, M., and Fonseca, E., 1990, Características geológicas petrológicas del contacto entre la asociación ofiolítica y el arco volcánico en Moa-Baracoa: Boletín De Geociencias, Centro Universitario De Pinar Del Río, Cuba, v. 1, p. 12–19.

Torró, L., Proenza, J.A., Farré De Pablo, J., Colomer, J.M., Garcia-Casco, A., Melgarejo, J.C., Alfonso, P., Gubern, A., Gallardo, E., Cazañas, X., Chávez, C., Del Carpio, R., León, P., Espaillat, J., and Lewis, J.F., 2015a, Mineralogy, geochemistry and sulfur isotope characterization of Cerro de Maimón (Dominican Republic), San Fernando and Antonio (Cuba) Lower Cretaceous VMS deposits: Formation during subduction initiation of the Proto-Caribbean lithosphere within a fore-arc: Ore Geology Reviews, (accepted).

Torró, L., Proenza, J.A., Garcia-Casco, A., Farré De Pablo, J., Del Carpio, R., León, P., Chávez, C., Domínguez, H., Brower, S., Espaillat, J., Nelson, C.E., and Lewis, J.F., 2015b, La geoquímica de la Formación Maimón (Cordillera Central, República Dominicana) revisada: Boletín Geológico y Minero, (in press).

Turner, S., Rushmer, T., Reagan, M., and Moyen, J.-F., 2014, Heading down early on? Start of subduction on Earth: Geology, v. 42, p. 139–142. doi:10.1130/G34886.1

Uysal, I., Kaliwoda, M., Karsli, O., Tarkian, M., Sadiklar, M.B., and Ottley, C.J., 2007, Compositional variations as a result of partial melting and melt–peridotite interaction in an upper mantle section from the Ortaca area, southwestern Turkey: The Canadian Mineralogist, v. 45, p. 1471–1493. doi:10.3749/canmin.45.6.1471

Wadge, G., Draper, G., and Lewis, J.F., 1984, Ophiolites of the northern Caribbean: A reappraisal of their roles in the evolution of the Caribbean plate boundary, *in* Gass, I.G., Lippard, S.J., and Shelton, A.W., eds., Ophiolites and Oceanic Lithosphere: Oxford, UK, Blackwell Scientific Publications, p. 367–380.

Whattam, S.A., and Stern, R.J., 2011. The 'subduction initiation rule': A key for linking ophiolites, intra-oceanic forearcs and subduction initiation: Contributions to Mineralogy and Petrology, v. 162, p. 1031–1045.

Whattam, S.A., and Stern, R.J., 2015, Late Cretaceous plume-induced subduction initiation along the southern margin of the Caribbean and NW South America: The first documented example with implications for the onset of plate tectonics: Gondwana Research, v. 27, p. 38–63. doi:10.1016/j.gr.2014.07.011

Whitney, D.L., and Evans, B.W., 2010, Abbreviations for names of rock-forming minerals: American Mineralogist, v. 95, p. 185–187. doi:10.2138/am.2010.3371

Wijbrans, J.R., Pringle, M.S., Koppers, A.A.P., and Scheveers, R., 1995, Argon geochronology of small samples using the Vulkaan argon laserprobe: Proc. Koninkl. Ned. Akad. Wetensch., v. 98, p. 185–218.

Winchester, J.A., and Floyd, P.A., 1977, Geochemical discrimination of different magma series and their differentiation products using immobile elements: Chemical Geology, v. 20, p. 325–343. doi:10.1016/0009-2541(77)90057-2

Workman, R.K., and Hart, S.R., 2005, Major and trace element composition of the depleted MORB mantle (DMM): Earth and Planetary Science Letters, v. 231, no. 1–2, p. 53–72. doi:10.1016/j.epsl.2004.12.005